Performance Analysis of Physical Layer Network Coding in Massive MIMO Systems with M-QAM Modulations

Bismark Okyere, Leila Musavian, and Rao Mumtaz

***Abstract*—In this paper, we develop a practical approach for deploying Physical Layer Network Coding (PNC) in multi-user M-Ary Quadrature Amplitude Modulation (M-QAM) Massive Multiple-Input Multiple-Output (MIMO) systems. We formulate a PNC mapping scheme as a function of clusters of estimated summation and difference (SD) of the transmitted symbols from user pairs. Utilizing existing linear detection schemes, such as Zero Forcing (ZF) and Minimum Mean Square Error (MMSE), a cluster of SD symbols are detected using an SD linearly transformed channel matrix. Furthermore, utilizing Maximum a Posteriori (MAP) soft decoding, the SD symbols are mapped to the PNC symbols, leveraging on the PNC symbol that maximizes the likelihood function. For each variant of M-QAM, we derive and simplify a specialization of the generalized PNC mapping function. The error performance results, through simulation, reveal that the proposed PNC scheme achieves twice the spectral efficiency in Massive MIMO, without changing the latter's underlying framework and without any degradation in the bit-error-rate (BER). In fact, our investigation has proved that the BER of the proposed Massive MIMO and PNC is slightly better than that of the conventional Massive MIMO. The feasibility of deploying our proposed PNC scheme in Massive MIMO systems paves way for NC applications to be realized in cellular systems.**

***Index Terms*—Massive MIMO, Physical Layer Network Coding, End-to-end simulation.**

I. Introduction

An insatiable demand for network capacity to support high data rate services such as high speed internet and multimedia applications has led to the evolution of the wireless communication systems. These evolved systems must provide solutions for not only future capacity constraints but also existing challenges, such as, network coverage, reliability, energy efficiency, latency and spectral efficiency. Some of these challenges can be addressed through the use of Massive Massive Multiple-Input Multiple-Output (MIMO) and Beamforming [1], [2]. Massive MIMO is an extension of the conventional MIMO and it exploits large array of antennas to spatially multiplex many users in the same time-frequency resource. This greatly improves the system capacity and throughput gains. Whilst the system capacity is boosted with large number of antennas, link reliability on the other hand, is improved through spatial diversity. Spatial diversity can be used to combat severe fading and improve reliability of wireless links by transmitting identical copies of the same information over multiple antennas. The large number of antennas yields extra degrees of freedom in space, which can be utilized to harness the available spatial resources. Massive MIMO, combined with Beamforming, is proven to improve spectral efficiency and to reduce the effects of interference [3]. By fine-tuning the phases and weights of the large multitude of antennas, interference is suppressed and coverage is extended by directing the radio waves to the desired user equipment (UE). These benefits have made Massive MIMO a compelling physical layer technology for the next generation of wireless access and considered as one of the key enablers in fifth generation (5G) of cellular communication systems [4].

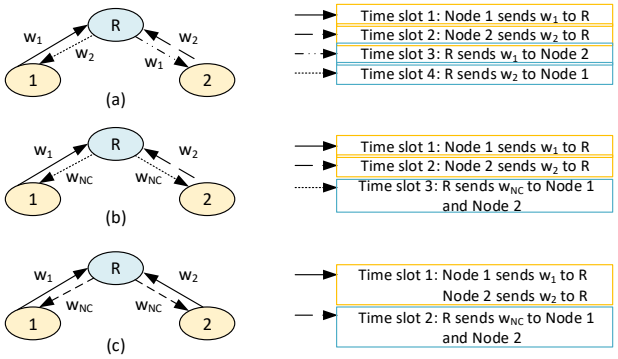

Fig. 1. Network Coding in TWRC

In-spite of all these illustrious benefits, Massive MIMO suffers from inter-cell and intra-cell interferences [5]. This makes Physical Layer Network Coding (PNC), another promising physical layer technique, compelling to explore in Massive MIMO systems. PNC is the application of well-known network coding technique [6] at the physical layer of the wireless network access [7]. Network coding, in itself, is a network layer coding technique that has seen its revolution from wireline to wireless access networks. It is a data dissemination paradigm in a distributed multi-hop relay network, where, instead of simply relaying the received packets, each node takes several packets and combines them together, and the combined packet is further transmitted in the network. Fig. 1 illustrates the operational concept of network coding in a two-way relay channel (TWRC) system model. The first system

Bismark Okyere and Leila Musavian are with the School of Computer Science and Electronic Engineering (CSEE), University of Essex, UK, Emails: {bismark.okyere, leila.musavian}@essex.ac.uk.

Rao Mumtaz is with GS-LDA in Aveiro, Portugal, Email: shmu@gs-lda.com.

Part of this work is already presented at the Globecom 2019, Hawaii, USA.

model shown in Fig. 1(a) is without network coding. Node 1 and Node 2 are not allowed to transmit at the same time, and therefore, it takes four time slots for messages, w_1 and w_2, to be exchanged. In Fig. 1(b), Node 1 and Node 2, much like in Fig. 1(a), transmit at orthogonal times. However, the relay, R, generates a combined message, w_{NC}, using w_1 and w_2, and sends w_{NC} in a single time slot back to Node 1 and Node 2. The bitwise XOR is typically the operation that generates w_{NC}, i.e., $w_{NC} = w_1 \oplus w_2$. In downlink (DL), each of these nodes performs a similar operation on w_{NC} by XOR'ring that with a copy of what was sent previously, i.e., $w_1 \oplus W_{NC}$ for Node 1, and $w_2 \oplus W_{NC}$ for Node 2, to extract the actual packet sent by the other node. In Fig. 1(c), Node 1 and Node 2 can transmit at the same time. Since messages w_1 and w_2 interfere at R, decoding or separating each from the other may not be possible. This is the reason wireless communication systems employ orthogonal multiple access schemes either in time, frequency or space to reduce the effects of interference. However, this interference becomes trivial through network coding at the physical layer since it generates or maps interfered symbols to network-coded (NC) symbols. The NC symbols are chosen such that there is no ambiguity for each node to recover its intended messages from others. Upon receiving the DL broadcast NC symbols, each node performs a similar operation, to retrieve the symbols sent by the other transmitting nodes. Irrespective of the chosen modulation scheme at the physical layer, the constellation of the superimposed signals at the relay may go out-of-range, if compared to the constellation of the modulated signals at the transmitting nodes. Therefore, a key challenge in PNC is the development of unambiguous PNC mapping algorithms that map superimposed constellations at the relay to the constellations that can be decoded by the nodes. The toleration of interference in PNC leads to capacity boost, as time slots required to have end-to-end communication in a relay system is reduced by half. Massive MIMO and PNC are two distinct physical layer techniques that can complement each other. The use of PNC in Massive MIMO systems can reduce the impact of multi-user interference. Massive MIMO suffers from intra-cell and inter-cell interference, albeit the enormous benefits it comes with. Signal processing techniques such as Zero Forcing (ZF), Minimum-Mean Square-Error (MMSE) and Maximum Ratio (MR) are some of the notable linear detectors that suppress interference in Massive MIMO systems, but they are sub-optimal [8] and require high signal-to-noise ratio (SNRs) to effectively null interference.

While recognising that there have been some works done in combining MIMO and PNC, to the best of our knowledge, none has produced any comprehensive study and results on the use of PNC in a multi-user Massive MIMO system, where the UEs transmit and receive with multi-antennas. In [9], the authors proposed a linear detection based scheme using log-likelihood ratio (LLR) and selective combining. The relay utilizes the summation and difference of the two end packets, and then converts them to an NC symbol. The focus of [9] was only a 2×2 MIMO with BPSK modulation. This work was then extended in [10] to a 4×4 MIMO relay system, where the relay is equipped with four antennas and two UEs, each equipped with two antennas. A multiplexing gain is observed when the number of antennas at both the relay and the two UEs increased in [10]. In [11], the authors proposed a space-time (ST) coded multiple-input multiple-output (MIMO) linear physical-layer network coding (LPNC) scheme that promises full-rate and full-diversity, while achieving the maximum coding gain of LPNC. An eigen-direction alignment precoding scheme is proposed in [12] and [13] for MIMO TWRCs, where multiple independent PNC streams are created over aligned eigenmodes. Although [14] did not focus on MIMO and PNC, they touched on combining channel coding and PNC to ensure network reliability, a key technique for practical deployment of MIMO and PNC. Therefore, in order for any proposed PNC scheme to be deployed in real systems, integrating channel coding [15] [16] is of utmost importance and further research is needed to ascertain the PNC performance. In [17], analog network coding based MIMO TWRC was investigated. However, this is known to propagate noise from a node to another, and therefore, its performance, is not as good as the schemes, where each node tries to detect the NC symbols from the noisy received symbols [18]. On the other hand, in [19]–[21], it was shown that, in a MIMO PNC scheme, when a user selects the strongest transmit antenna, it significantly outperforms space-time block codes. A channel-quantized PNC, that converts K received signals at the relay into two signals by a QR matrices decomposition in a MIMO TWRC, where Q is an orthogonal matrix and R, an upper triangular matrix, is proposed in [22], which showed that PNC technique can achieve full diversity gain of K. A Full-duplex TWRC in Massive MIMO together with a lattice-based PNC was investigated in [23], which showed that their proposed scheme requires just a single timeslot to exchange information across TWRC using full-duplexing, where transmission and reception can occur at the same time in a single node. However, most practical communication systems still operate in half-duplexing mode. Looking at the previous works, none has produced any result for a joint Multi-user Massive MIMO and PNC, with more than 2 UEs and where each UE can have multiple number of antennas. To the best of our knowledge, this is the first attempt to implement M-Ary Quadrature Amplitude Modulation (M-QAM) for a multi-user PNC-Massive MIMO.

We recall that Massive MIMO with PNC achieves twice spectral efficiency when compared with traditional Massive MIMO schemes. We previously demonstrated this in [27]. We presented the concept of using SD scheme to combine PNC and Massive MIMO. We presented the mathematical derivations of the PNC mapping function, employing log-likelihood ratio (LLR), however, the focus was only on QPSK modulation. The order of the modulation scheme is important in assessing the complexity of the PNC mapping in Massive MIMO systems. We presented the error performance analysis of the joint Massive MIMO and PNC system model with QPSK modulation and showed how he SD symbols are estimated through ZF and MMSE detection. The proposed PNC mapping function in [27] can only work for Massive MIMO with QPSK transmission, and therefore, a generalization of the mathematical derivation for the PNC mapping function

is required. The generalized PNC mapping function will 1) provide a common platform for any M-QAM modulation scheme to be investigated and utilized, and 2) understand the complexity and optimizations required for the PNC mapping function, particularly, for higher order modulation schemes.

In this paper, we present a generic approach where PNC can be deployed in Massive MIMO systems that utilizes any variant of M-QAM and without changing the underlying Massive MIMO framework. This further allows existing detection schemes such as ZF and MMSE to be used without any modification. The proposed scheme requires a linear transformation of the channel utilizing an adopted sum-difference (SD) matrix. The goal of the SD matrix transformation of the channel is to create clusters, each of a pair of detected SD symbols, and where these pairs of SD symbols are later mapped to PNC symbols. The detection of the SD symbols is accomplished with the equalization matrix. For the clustering to function effectively, the equalization matrix has to be based on the SD-transformed channel matrix. Therefore, in this work, we investigate the error performance of the detection of the SD symbols and the PNC mapping, which can provide guidelines for the design of efficient MIMO-based communication systems using PNC. We summarize our contributions as follows:

- We demonstrate the feasibility of deploying PNC in Massive MIMO systems, where M-QAM modulation is the transmission scheme, while the underlying detection schemes for MIMO without PNC remain the same.
- For uplink transmissions, we design a PNC mapping scheme based on a SD transformation of the channel. The proposed scheme reduces the complexity of performing network coding at the physical layer.
- We formulate a generalized PNC mapping function, for which its inputs are the detected SD symbols from the clusters derived from the SD transformation of the channel and equalization of the received superimposed symbols. Furthermore, we derive and optimize a specialization of the generalized PNC mapping function and demonstrate that with a few variants of the M-QAM.
- Finally, we evaluate the bit-error-rate (BER) of the detection of the SD symbols with ZF and MMSE and the PNC mapping performance of this scheme.

II. Proposed Relay System of PNC in Massive MIMO

It is the aim of this section to present the system model and its parameters, and to explain how PNC can be deployed in Massive MIMO systems with M-QAM modulations. We re-introduce the SD scheme, initially proposed in [27], and then present a generalized mathematical formulation for the PNC mapping functions for all order of dimensions of the QAM modulation scheme.

A. System Model

We consider a single cell Massive MIMO, in which N users exchange information through a BS, as in Fig. 2. Each of the N UEs is equipped with up to K antennas, and the BS with

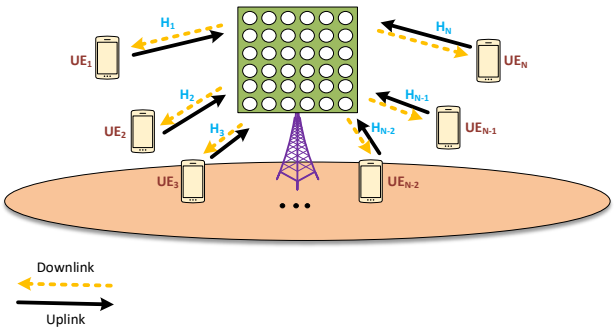

Fig. 2. System Model for Massive MIMO and PNC

M antennas. The communication among all UEs is done in the same time-frequency resource, and therefore, interference is expected, which is a common assumption in Massive MIMO systems, even without network coding. It is assumed that $M \geq 64$, $M \gg N$, $M \gg K$ in order to fulfil the universal antenna requirements of Massive MIMO, where $\gg$ denotes far greater than. The system model is also assumed to operate in half-duplex, in the sense that, each UE cannot transmit and receive at the same time. Therefore, each round of information exchange consists of two phases, namely, uplink (UL) and downlink (DL) phases. In the DL, the mapped PNC symbols are delivered to the UEs.

Asynchronisation of transmission and reception of the interfered symbols is one the major issues in PNC. It is also one of the main research areas with respect to PNC. Loss in synchronisation impacts the performance in estimating the PNC symbols, as most PNC algorithms assume that all transmitted symbols will arrive at the same time at the receiver. However, for the sake of simplicity, in our work, we assume synchronous transmission, hence, in the UL phase, all users transmit to the BS simultaneously in the same frequency band and at the same time. We also did not consider channel coding in this work for the sake of simplicity, considering there already have been some works [14] in combining channel coding and PNC, as previously stated in the introduction section. In essence, channel coding is essential for improving the reliability of the PNC scheme in practical systems. It is already established that if the sources transmitting in the UL phase use a uniform channel code, then the codeword as a result of XOR'ing of the sources symbols is still valid. Although there is no direct XOR'ing in our proposed scheme, we believe some of the existing joint channel coding PNC schemes can be tailored and extended to our proposed PNC scheme.

Let $\boldsymbol{H}$ be the overall channel between the BS and the multi-antenna UEs in the multi-user Massive MIMO system. As depicted in Fig. 2, $\boldsymbol{H}$ can be formulated as

$$\boldsymbol{H} = \begin{bmatrix} \boldsymbol{H}(1) & \boldsymbol{H}(2) & \dots & \boldsymbol{H}(N) \end{bmatrix}_{\mathrm{M \times L}}, \tag{1}$$

where $L = K \times N$, and $\boldsymbol{H}(n)$ for $n = 1, \dots, N$, is the $M \times K$ channel matrix between the BS and the n^{th} UE and can be

expressed as

$$\boldsymbol{H}(n) = \begin{bmatrix} h(n)_{1,1} & h(n)_{1,2} & \dots & h(n)_{1,k} \\ h(n)_{2,1} & h(n)_{2,2} & \dots & h(n)_{2,k} \\ \vdots & \vdots & \ddots & \vdots \\ h(n)_{m,1} & h(n)_{m,2} & \dots & h(n)_{m,k} \end{bmatrix}_{\mathrm{M\times K}}, \quad (2)$$

where $h(n)_{m,k} \in \mathbb{C}$, for $m = 1, \dots, M$ and $k = 1, \dots, K$, denotes the complex channel gain between m^{th} antenna of BS and k^{th} antenna of the n^{th} UE. The entries of $h(n)_{m,k}$ are assumed to be identically and independently distributed (i.i.d.) complex Gaussian, distributed with zero mean and unit variance, presented by $\mathcal{CN}(0, 1)$. The received signal vector at the BS is given by

$$\boldsymbol{r} = \boldsymbol{H}\boldsymbol{s} + \boldsymbol{z}, \quad (3)$$

where $\boldsymbol{r} \in \mathbb{C}^{M\times 1}$ is the received symbols vector, $\boldsymbol{z} \in \mathbb{C}^{M\times 1}$ the vector of additive white Gaussian noise (AWGN) at the receive antennas of the BS, with zero mean and variance of σ^2, i.e., $\mathcal{CN}(0, \sigma^2)$, and $\boldsymbol{s} \in \mathbb{C}^{L\times 1}$, is the overall transmitted symbols vector from all the UEs. The transmitted symbols vector, $\boldsymbol{s}$, can further be expressed as

$$\boldsymbol{s} = \begin{bmatrix} \boldsymbol{s}(1) & \boldsymbol{s}(2) & \dots & \boldsymbol{s}(n) \end{bmatrix}^{\mathrm{T}}_{1\times \mathrm{L}}, \quad (4)$$

where $\boldsymbol{s}(n) = \begin{bmatrix} s_1 & s_2 & \dots & s_K \end{bmatrix}^{\mathrm{T}}_{1\times \mathrm{K}}$ represents a vector of K symbols from the n^{th} UE.

In general, a MIMO detector is required to estimate transmitted symbols vector $\boldsymbol{s}$ from the received symbols vector $\boldsymbol{r}$. Linear detectors such as ZF and MMSE are known to have desirable computational complexity, but suffer from an ample performance loss in comparison to the Maximum Likelihood (ML), and they are, therefore, considered sub-optimal compared to ML. However, they both have been proven to perform well in Massive MIMO [28]. They are, therefore, employed in this paper. This goes without saying that the performance loss using these linear detectors compared to ML is not considered in this paper. We are convinced, by looking at our algorithm, that these linear detectors can be replaced by other high performing sub-optimal detectors, and the performance of our PNC scheme will scale accordingly.

Applying the aforementioned linear detectors with an $M \times N$ detection matrix $\boldsymbol{G}$ to the received signal vector $\boldsymbol{r}$, the estimate of the transmit symbols vector $\boldsymbol{s}$ can be expressed as

$$\widehat{\boldsymbol{s}} = \boldsymbol{G}\boldsymbol{r}, \quad (5)$$

where $\boldsymbol{G}$, respectively, for ZF and MMSE, is

$$\boldsymbol{G}^{\mathrm{ZF}} = (\boldsymbol{H}^{\mathrm{H}}\boldsymbol{H})^{-1}\boldsymbol{H}^{\mathrm{H}}, \quad (6)$$

$$\boldsymbol{G}^{\mathrm{MMSE}} = (\boldsymbol{H}^{\mathrm{H}}\boldsymbol{H} + \sigma^2\mathrm{I})^{-1}\boldsymbol{H}^{\mathrm{H}}, \quad (7)$$

where $(\cdot)^{\mathrm{H}}$, $(\cdot)^{-1}$, respectively, are the conjugate transpose and inverse and, $\boldsymbol{I}$, is the identity Matrix of the same dimension as $\boldsymbol{H}$. It has to be noted that in practice, the noise variance varies from one antenna to the other in the same node. Also, for the sake of simplicity, we assume that there is a perfect channel state information (CSI) at the receiver, and therefore, $\boldsymbol{H}$ is known at the BS.

The goal now is to derive NC symbols from the received superimposed transmitted symbols at the BS, without decoding them individually. The Massive MIMO system model fairly tolerates interference, a key requirement for PNC, and therefore, moving the network coding to the physical layer is a means to gaining advantages of both approaches, by jointly performing PNC and Massive MIMO detection. Furthermore, in order for PNC to be deployed in mainstream cellular Massive MIMO systems, it is essential that it supports M-QAM modulation. Adaptive modulation and coding, which based on the channel quality, the BS assigns a suitable modulation and coding scheme to the UEs, is a key transmission scheme in cellular systems. The chosen Adaptive modulation and coding scheme has to have the desired balance of spectral efficiency and error resilience for the link state as observed by the device. In [27], we derived the PNC mapping functions using the SD scheme, but the solution was tied to QPSK modulation. It is imperative that the solution is generalized for all variants of M-QAM modulations for the reasons just mentioned above. The most important criteria for PNC is that the PNC mapping function, $f_{\mathrm{PNC}}(.)$, used at the BS, should generate PNC symbols that can be decoded by the UEs without any ambiguity in recovering the symbols from the other users.

Each of the antennas at the Massive MIMO BS receives superimposed symbols that constitute transmitted symbols from each of the multi-antenna UEs. The constellation for the received interfered symbols, depending on the modulation scheme used at the UEs, may lead to ambiguities if they are mapped to NC symbols, which follow the same constellation as the transmitted symbols. A practical solution in alleviating this network coding ambiguity in Massive MIMO systems is, by creating clusters, which constitute of a few transmitted symbols and whose superposition are independently passed on to $f_{\mathrm{PNC}}(.)$, to generate the NC symbols. An SD matrix transformation of the Massive MIMO channel is a plausible means of creating these kind of clusters. In order to extend the SD scheme in our earlier work in [27] to all variants of M-QAM, a top-down approach is employed in this paper, where the scheme is first, generalized, and then based on the modulation scheme of interest, further optimizations are embarked upon. An SD transformation of the Massive MIMO channel, hereafter, referred to as Massive SD transformation, transforms the channel, $\boldsymbol{H}$, with a massive SD Matrix, $\boldsymbol{P}_{\mathrm{sd}}$, which is expressed as

$$\boldsymbol{P}_{\mathrm{sd}} = \begin{bmatrix} \boldsymbol{I}_{\mathrm{Q}} & \boldsymbol{I}_{\mathrm{Q}} \\ \boldsymbol{I}_{\mathrm{Q}} & -\boldsymbol{I}_{\mathrm{Q}} \end{bmatrix}_{\mathrm{L\times L}}, \quad (8)$$

where $L = K \times N$, $Q = \frac{1}{2}L$ and $\boldsymbol{I}_{\mathrm{Q}}$ denoting a $Q \times Q$ square Identity Matrix. The inverse, $\boldsymbol{P}_{\mathrm{sd}}^{-1}$, is related to $\boldsymbol{P}_{\mathrm{sd}}$ as, $\boldsymbol{P}_{\mathrm{sd}}^{-1} = \frac{1}{2}\boldsymbol{P}_{\mathrm{sd}}$. The received signal, given in (3), hence, can be reformulated as

$$\boldsymbol{r} = (\boldsymbol{H}{\boldsymbol{P}_{\mathrm{sd}}}^{-1})(\boldsymbol{P}_{\mathrm{sd}}\boldsymbol{s}) + \boldsymbol{z} \quad (9)$$

$$= \boldsymbol{H}_{\mathrm{sd}}\boldsymbol{s}_{\mathrm{sd}} + \boldsymbol{z}, \quad (10)$$

where $\boldsymbol{H}_{\text{sd}} = \frac{1}{2}\boldsymbol{H}\boldsymbol{P}_{\text{sd}}$, is the linear transformation of the Massive MIMO channel with a Massive SD matrix, and $\boldsymbol{s}_{\text{sd}} = \boldsymbol{P}_{\text{sd}}\boldsymbol{s}$, clusters of SD symbols, whose estimates at the BS, are then mapped to the PNC symbols. The reason for adopting the SD matrix (in (8)) in our scheme is that, this matrix provides a set of correlated sum and difference of pairs of transmitted symbols, and in turn, the PNC symbols can effectively be derived from these SD symbols. Furthermore, its property of being a factor of its inverse, preserves the received symbols vector, $\boldsymbol{r}$, as in (9) and (10), facilitating the adoption of ZF and MMSE without any modification, to detect SD symbols directly from the received symbols vector, $\boldsymbol{r}$. Each pair of the detected SD symbols forms a cluster and this cluster becomes the input to the PNC mapping function, $f_{\text{PNC}}(.)$, to generate the corresponding PNC symbols. The pair of estimated SD symbols in each cluster, is then passed on to the PNC mapping function, $f_{\text{PNC}}(.)$, to generate the corresponding PNC symbols.

Since $\boldsymbol{r}$, the received symbols vector, in either (3) or (10) is assumed to be received over a fading channel, it is imperative that $\boldsymbol{s}_{\text{sd}}$ is estimated. Leveraging on Massive MIMO linear detectors such as, ZF and MMSE, the estimate of $\boldsymbol{s}_{\text{sd}}$, at the BS, by extending (5)-(7), is expressed as

$$\widehat{\boldsymbol{s}}_{\text{sd}} = \boldsymbol{G}_{\text{sd}}\boldsymbol{r} \ , \tag{11}$$

where $\boldsymbol{G}_{\text{sd}}$ is the SD equalization matrix. The SD equalization matrix is based on the massive SD-transformed channel matrix, $\boldsymbol{H}_{\text{sd}}$, and for ZF and MMSE, it is expressed as

$$\boldsymbol{G}_{\text{sd}} = \begin{cases} (\boldsymbol{H}_{\text{sd}}{}^{\text{H}}\boldsymbol{H}_{\text{sd}})^{-1}\boldsymbol{H}_{\text{sd}}{}^{\text{H}}, & \text{for ZF} \\ (\boldsymbol{H}_{\text{sd}}{}^{\text{H}}\boldsymbol{H}_{\text{sd}} + \sigma^2\text{I})^{-1}\boldsymbol{H}_{\text{sd}}{}^{\text{H}}, & \text{for MMSE} \end{cases} . \tag{12}$$

Upon receiving $\boldsymbol{r}$ from multiple UEs, knowing $\boldsymbol{H}$, the BS can determine $\boldsymbol{G}_{\text{sd}}$, and then, use that to estimate the $L \times 1$ clusters of SD of the transmitted symbols. The clusters of the estimated SD symbols at the BS is expressed as

$$\widehat{\boldsymbol{s}}_{\text{sd}} = \begin{bmatrix} \widehat{s}_{\text{sd},1} \\ \widehat{s}_{\text{sd},2} \\ \vdots \\ \widehat{s}_{\text{sd},\text{Q}} \\ \widehat{s}_{\text{sd},\text{Q+1}} \\ \vdots \\ \widehat{s}_{\text{sd},2\text{Q}} \end{bmatrix} = \begin{bmatrix} s_1 + s_{\text{Q+1}} \\ s_2 + s_{\text{Q+2}} \\ \vdots \\ s_{\text{Q}} + s_{2\text{Q}} \\ s_1 - s_{\text{Q+1}} \\ \vdots \\ s_{\text{Q}} - s_{2\text{Q}} \end{bmatrix}_{\text{L}\times 1} , \tag{13}$$

where for example, $\widehat{s}_{\text{sd},1}$ and $\widehat{s}_{\text{sd},\text{Q+1}}$, are respectively, the estimated summation and difference of the transmitted symbols, s_1 and $s_{\text{Q+1}}$. This pair of SD symbols constitutes a cluster, that is then, passed on to the PNC mapping, $f_{\text{PNC}}(.)$. For these clusters of summation and difference symbols to be created as in (13), the BS has to view the multi-user Massive MIMO system model as a giant point-to-point Massive MIMO between itself and a black box of many multi-antenna UEs. The dimension of the massive SD-transformed channel matrix, $\boldsymbol{H}_{\text{sd}}$, is assumed to be a square matrix, for the sake of simplicity.

Finally, a vector of the PNC symbols, $\widehat{\boldsymbol{s}}_{\text{PNC}}$, is generated from the PNC mapping function, $f_{\text{PNC}}(.)$, through the relation

$$\widehat{\boldsymbol{s}}_{\text{PNC}} = f_{\text{PNC}}(\widehat{\boldsymbol{s}}_{\text{sd}}) \tag{14}$$

$$= \begin{bmatrix} f_{\text{PNC}}(\widehat{s}_{\text{sd},1}, \widehat{s}_{\text{sd},\text{Q+1}}) \\ f_{\text{PNC}}(\widehat{s}_{\text{sd},2}, \widehat{s}_{\text{sd},\text{Q+2}}) \\ \vdots \\ f_{\text{PNC}}(\widehat{s}_{\text{sd},\text{Q}}, \widehat{s}_{\text{sd},2\text{Q}}) \end{bmatrix}_{\text{Q}\times 1} . \tag{15}$$

The next section will describe the underlying scheme for the PNC mapping function, $f_{\text{PNC}}(.)$.

B. Generalization of the PNC Mapping Scheme

The goal of the PNC mapping scheme is to derive the set of PNC symbols, $\widehat{\boldsymbol{s}}_{\text{PNC}}$, from the estimated massive SD transmitted symbols, $\widehat{\boldsymbol{s}}_{\text{sd}}$. The derived PNC symbols, $\widehat{\boldsymbol{s}}_{\text{PNC}}$, must not lead to any ambiguity of decoding, if broadcast in DL to the UEs. If the probability distribution function is known, Maximum a Posteriori (MAP) decoder can be employed to derive $\widehat{\boldsymbol{s}}_{\text{PNC}}$. By definition,

$$\text{Posteriori} = \frac{\text{Likelihood} \times \text{Prior}}{\text{Observation}} . \tag{16}$$

Assuming the unknown or the parameter to be estimated is θ, and x, the observed data, then (16) can be expressed in these variables as

$$P(\theta|x) = \frac{P(x|\theta)P(\theta)}{P(x)} , \tag{17}$$

where $P(\theta|x)$ is the posteriori or the conditional probability of the unknown, θ, given the observation, x, whereas $P(x|\theta)$ is the likelihood or the conditional probability of the observation given the unknown, and $P(\theta)$ and $P(x)$ are respectively, the marginal distribution functions for the unknown and the observation.

A MAP decoder is based on (17), and can be formulated as determining the value of the parameter, θ, that maximizes the posteriori, $P(\theta|x)$. This can be expressed as

$$\widehat{\theta}_{\text{MAP}} = \underset{\theta}{\text{argmax}} \ P(\theta|x) \tag{18}$$

$$= \underset{\theta}{\text{argmax}} \ \frac{P(x|\theta)P(\theta)}{P(x)} . \tag{19}$$

Since $P(x)$ is not a function of θ, it can be ignored, and therefore, the $\widehat{\theta}_{\text{MAP}}$ can be approximated to

$$\widehat{\theta}_{\text{MAP}} \approx \underset{\theta}{\text{argmax}} \ P(x|\theta)P(\theta) . \tag{20}$$

Again, $P(\theta)$ can be ignored if the expected values of θ that maximizes the posteriori distribution function are each equally likely. Hence, $P(\theta)$ becomes a constant, and therefore, can be ignored, leading (20) to further be approximated as

$$\widehat{\theta}_{\text{MAP}} \approx \underset{\theta}{\text{argmax}} \ P(x|\theta) = \widehat{\theta}_{\text{MLE}} , \tag{21}$$

where $\widehat{\theta}_{\text{MLE}}$ is the Maximum Likelihood Estimator (MLE). When the cardinality of θ is 2, hypothesis testing using LLR is plausible. If the cardinality is more than 2, then LLR is not the appropriate approach.

Having defined the MAP decoder, we can now employ it in our PNC Mapping scheme in Massive MIMO systems in estimating the NC symbols at the physical layer. In (13), clusters of estimated SD symbols that are mapped to PNC symbols are expressed as $\{(\widehat{s}_{\text{sd,i}}, \widehat{s}_{\text{sd,Q+i}}) \mid 1 \leq i \leq Q\}$. We assume that the corresponding set of clusters of transmitted input symbol, $\{(s_i, s_{Q+i}) \mid 1 \leq i \leq Q, s_i, s_{Q+i} \in \Theta\}$, are modulated symbols from the constellation, represented by Θ. Then, the Likelihood of obtaining the PNC symbol, $\widehat{s_i \oplus s_{Q+i}} = v$, such that $v \in \Theta$ is expressed as in (22), Since the noise in (3) and (10) is assumed to be AWGN, the likelihood function can be assumed to be Gaussian. Using the Gaussian probability density function, $P(Y) = \dfrac{1}{\sqrt{2\pi\sigma^2}} e^{-\dfrac{(y-\mu)^2}{2\sigma^2}}$, where y is the received symbol, μ the expected value of the combined input symbols and σ^2, the noise variance, (22) can be expressed further as in (23).

Knowing the general Likelihood's function for the set of all clusters, $L(\widehat{s_i \oplus s_{Q+i}} = v | \widehat{s}_{\text{sd,i}}, \widehat{s}_{\text{sd,Q+i}})$, the MAP estimator in (20) can be employed to determine the PNC symbol of each cluster as follows

$$(\widehat{s_i \oplus s_{Q+i}} = v)_{MAP} \approx \underset{\widehat{s_i \oplus s_{Q+i}}}{\operatorname{argmax}} \; L(\widehat{s_i \oplus s_{Q+i}} = v | \widehat{s}_{\text{sd,i}}, \widehat{s}_{\text{sd,Q+i}}) P(\widehat{s}_{\text{sd,i}}, \widehat{s}_{\text{sd,Q+i}}). \tag{24}$$

The overall set of estimated PNC symbols is expressed as

$$\widehat{s}^{\,i}_{\text{PNC}} = f_{\text{PNC}}(\widehat{s}_{\text{sd,i}}, \widehat{s}_{\text{sd,Q+i}}) \tag{25}$$

$$= \{(s_i \oplus \widehat{s_{Q+i}} = v)_{\text{MAP}} \mid 1 \leq i \leq Q, \; v \in \Theta\}. \tag{26}$$

In the next section, we will provide details into how the generalized MAP-based PNC mapping function in (23) - (26) is applied to a few variants of the M-QAM modulation scheme.

C. Specialization of the PNC Mapping scheme for 4-QAM

This section describes the application of the PNC Mapping scheme in subsection II-B to Massive MIMO system where the transmissions from the UEs use lower-order modulation, such as 4-QAM. We will demonstrate by focusing on a single cluster of estimated SD symbols, $\widehat{\boldsymbol{s}}_{\text{sd,i}}$ and $\widehat{\boldsymbol{s}}_{\text{sd,Q+i}}$, derived from the equalization of the received symbol vector $\boldsymbol{r}$, using massive SD equalization matrix (see (11)-(12)). For the sake of simplicity, we will focus on only the in-phase (I) component constellation of QPSK. However, since quadrature (Q) component of QPSK is similar to the I-component and independently modulated or demodulated, the PNC mapping of the I-component is equally applicable to the Q-component. Table I shows how SD symbols, $\boldsymbol{s}_{\text{sd,i}}$ and $\boldsymbol{s}_{\text{sd,Q+i}}$, of the transmitted symbols, $\boldsymbol{s}_i$ and $\boldsymbol{s}_{Q+i}$, are mapped to the PNC symbols, $\boldsymbol{s}^{\,i}_{\text{PNC}}$. Having $\boldsymbol{s}_{\text{sd,i}}$ and $\boldsymbol{s}_{\text{sd,Q+i}}$ in Table I as the expected SD symbols, $f_{\text{PNC}}(.)$ function presented in subsection II-B, can then be used to estimate the PNC symbols from the estimated SD symbols, $\widehat{\boldsymbol{s}}_{\text{sd,i}}$ and $\widehat{\boldsymbol{s}}_{\text{sd,Q+i}}$. In [27], we presented an approximation of $f_{\text{PNC}}(.)$ for QPSK in a Massive MIMO system. This approximation also applies to 4-QAM. For brevity, we will revisit the derivations without all the detailed simplification. Since the targeted PNC symbols' constellation for either in-phase (I) or quadrature (Q) component of 4-QAM is $\Theta_{4-QAM} = \{+1, -1\}$, and the cardinality of Θ_{4-QAM} is 2, LLR based on the MAP decoder in (24) is the preferred, as it is a compact approach to estimate the PNC symbols. This can be expressed as in (27), where

$$LL_{Q+i}(s_i \oplus s_{Q+i} = +1) = \ln\left(\frac{e^{\frac{2\widehat{s}_{\text{sd,Q+i}} - 2}{\sigma^2_{Q+i}}}}{e^{\frac{2\widehat{s}_{\text{sd,Q+i}} - 2}{\sigma^2_{Q+i}}} + e^{-\frac{2\widehat{s}_{\text{sd,Q+i}} - 2}{\sigma^2_{Q+i}}}}\right), \tag{28}$$

and

$$LL_i(s_i \oplus s_{Q+i} = -1) = \ln\left(\frac{e^{\frac{2\widehat{s}_{\text{sd,i}} - 2}{\sigma^2_i}}}{e^{\frac{2\widehat{s}_{\text{sd,i}} - 2}{\sigma^2_i}} + e^{-\frac{2\widehat{s}_{\text{sd,i}} - 2}{\sigma^2_i}}}\right), \tag{29}$$

and where ${\sigma_i}^2 = \{\boldsymbol{G}^{\text{H}}_{\text{sd}} \boldsymbol{G}_{\text{sd}}\}_{i,i}\sigma^2$ is the noise variance of the i^{th} stream upon estimation of the SD symbols. To reduce the computational complexity, (28) and (29) can be approximated using the log sum of exponential property [29], i.e. $\ln(e^x + e^y) \approx \max(x, y) + \ln(1 + e^{-|x-y|})$, where $\max(x, y)$ is the maximum value of the two variables, x and y. Equations (28) and (29) are, hence, approximated as in (30) and (31), respectively.

By definition, $LLR(s_i \oplus s_{Q+i}) \geq 0$, and therefore the estimated PNC symbols is expressed as in (32).

D. Specialization of the PNC Mapping for 16-QAM

Having already presented the PNC Mapping scheme for 4-QAM modulation in Massive MIMO system, this section will focus on relatively a higher order modulation scheme, such as 16-QAM. The constellation for each of I/Q component of 16-QAM is $\Theta_{16-QAM} = \{-3, -1, 1, 3\}$. As in previous section, the goal is to estimate PNC symbols, $\widehat{\boldsymbol{s}}^{\,i}_{\text{PNC}}$, from the estimated SD symbols, $\widehat{\boldsymbol{s}}_{\text{sd,i}}$ and $\widehat{\boldsymbol{s}}_{\text{sd,Q+i}}$, and the expected SD symbols, $\boldsymbol{s}_{\text{sd,i}}$ and $\boldsymbol{s}_{\text{sd,Q+i}}$, in Table II, using the $f_{\text{PNC}}(.)$ function, assuming that the transmitted symbols are based on 16-QAM.

Since the cardinality of Θ_{16-QAM} is more than 2, LLR is not the appropriate approach in estimating the PNC symbols, contrary to the approach for 4-QAM in subsection II-C, where the cardinality is 2. The estimated PNC symbol, based on MAP decoder, for each cluster is given in generalized equation (24). In this equation, the prior joint probability distribution, $P(\widehat{s}_{\text{sd,i}}, \widehat{s}_{\text{sd,Q+i}})$, of estimated SD symbols, $\widehat{s}_{\text{sd,i}}$ and $\widehat{s}_{\text{sd,Q+i}}$, is equally likely, and therefore the (24) approximates to an MLE i.e.

$$(\widehat{s_i \oplus s_{Q+i}} = v)_{MAP} = (\widehat{s_i \oplus s_{Q+i}} = v)_{MLE} \tag{33}$$

$$\approx \underset{\widehat{s_i \oplus s_{Q+i}}}{\operatorname{argmax}} \; L(\widehat{s_i \oplus s_{Q+i}} = v | \widehat{s}_{\text{sd,i}}, \widehat{s}_{\text{sd,Q+i}}) \; . \tag{34}$$

$$L(s_i \widehat{\oplus\, s_{Q+i}} = v|\widehat{s}_{\text{sd,i}}, \widehat{s}_{\text{sd,Q+i}}) = \sum_{v\in\Theta} P(\widehat{s}_{\text{sd,i}}, \widehat{s}_{\text{sd,Q+i}}|s_i \widehat{\oplus\, s_{Q+i}} = v)$$
$$= \sum_{v\in\Theta} P(\widehat{s}_{\text{sd,i}}|s_i \widehat{\oplus\, s_{Q+i}} = v) P(\widehat{s}_{\text{sd,Q+i}}|s_i \widehat{\oplus\, s_{Q+i}} = v) \ . \quad (22)$$

$$L(s_i \widehat{\oplus\, s_{Q+i}} = v|\widehat{s}_{\text{sd,i}}, \widehat{s}_{\text{sd,Q+i}}) = \sum\nolimits_{v\in\Theta} \frac{1}{2\pi\sqrt{\sigma_i^2\sigma_{Q+i}^2}} e^{-\frac{\left(\widehat{s}_{\text{sd,i}} - s_{\text{sd,i}}\right)^2}{2\sigma_i^2}} e^{-\frac{\left(\widehat{s}_{\text{sd,Q+i}} - s_{\text{sd,Q+i}}\right)^2}{2\sigma_{Q+i}^2}} \ . \quad (23)$$

TABLE I
PNC MAPPING OF I/Q-COMPONENT OF 4-QAM, BASED ON SD SCHEME

$\boldsymbol{s}_i$	$\boldsymbol{s}_{Q+i}$	$\boldsymbol{s}_{\text{sd,i}}$	$\boldsymbol{s}_{\text{sd,Q+i}}$	$\boldsymbol{s}_{\text{PNC}}^{i}$
1	1	2	0	-1
1	-1	0	2	1
-1	1	0	-2	1
-1	-1	-2	0	-1

$$LLR(s_i \oplus s_{Q+i}) = \ln\left[\frac{L(s_i \widehat{\oplus\, s_{Q+i}} = +1|\widehat{s}_{\text{sd,i}}, \widehat{s}_{\text{sd,Q+i}}) P(\widehat{s}_{\text{sd,i}}, \widehat{s}_{\text{sd,Q+i}})}{L(s_i \widehat{\oplus\, s_{Q+i}} = -1|\widehat{s}_{\text{sd,i}}, \widehat{s}_{\text{sd,Q+i}}) P(\widehat{s}_{\text{sd,i}}, \widehat{s}_{\text{sd,Q+i}})}\right]$$
$$= \ln\left[\frac{P(\widehat{s}_{\text{sd,i}}|s_{\text{sd,i}} = 0) P(\widehat{s}_{\text{sd,Q+i}}|s_{\text{sd,Q+i}} = -2) + P(\widehat{s}_{\text{sd,i}}|s_{\text{sd,i}} = 0) P(\widehat{s}_{\text{sd,Q+i}}|s_{\text{sd,Q+i}} = +2)}{P(\widehat{s}_{\text{sd,Q+i}}|s_{\text{sd,Q+i}} = 0) P(\widehat{s}_{\text{sd,i}}|s_{\text{sd,i}} = -2) + P(\widehat{s}_{\text{sd,Q+i}}|s_{\text{sd,Q+i}} = 0) P(\widehat{s}_{\text{sd,i}}|s_{\text{sd,i}} = +2)}\right]$$
$$= LL_{Q+i}(s_i \oplus s_{Q+i} = +1) - LL_i(s_i \oplus s_{Q+i} = -1) \ . \quad (27)$$

The 16-QAM PNC symbol, $v \in \Theta_{16-QAM}$, given the estimated SD symbols, $\widehat{s}_{\text{sd,i}}$ and $\widehat{s}_{\text{sd,Q+i}}$, that maximizes the likelihood function, $L(s_i \widehat{\oplus\, s_{Q+i}} = v|\widehat{s}_{\text{sd,i}}, \widehat{s}_{\text{sd,Q+i}})$, becomes the estimated PNC symbol, $(s_i \widehat{\oplus\, s_{Q+i}} = v)_{MAP}$. Given the expected SD symbols and the PNC symbols that they are mapped to in Table II, the log-likelihood of PNC symbol of -3, given that the cluster has the estimated SD symbols, $\widehat{s}_{\text{sd,i}}$ and $\widehat{s}_{\text{sd,Q+i}}$, is expressed as in (35). The log-likelihood of PNC symbol of -1, given $\widehat{s}_{\text{sd,i}}$ and $\widehat{s}_{\text{sd,Q+i}}$, is expressed as in (36). The log-likelihood of PNC symbol of +1, given $\widehat{s}_{\text{sd,i}}$ and $\widehat{s}_{\text{sd,Q+i}}$, is expressed as in (37). Finally, the log-likelihood of PNC symbol of +3, given $\widehat{s}_{\text{sd,i}}$ and $\widehat{s}_{\text{sd,Q+i}}$, is expressed as in (38).

In all of these, four sets of the sum, $\widehat{s}_{\text{sd,i}}$ and the difference, $\widehat{s}_{\text{sd,Q+i}}$, influenced the Gaussian distribution function for the corresponding LL. So for example, to estimate the PNC Symbol +3, the following sets of $\{\widehat{s}_{\text{sd,i}}, \widehat{s}_{\text{sd,Q+i}}\} = \{0, 2\}, \{0, -2\}, \{0, 6\}, \{-6, 0\}$ were utilized in LL as shown in (38). This approach has to be repeated for other PNC symbols.

III. NUMERICAL RESULTS

In this section, we present Monte-Carlo system simulation results to evaluate the performance of the proposed PNC mapping scheme for Massive MIMO systems. The goal of the simulation is to evaluate the Bit-Error-Rate (BER) of the MAP-based PNC mapping functions derived in sub-section II-C and sub-section II-D, using linear detectors, such as ZF and MMSE, to estimate the clusters of SD symbols.

A. Simulation Setup

Simulation parameters are listed in Table III. The simulation scenario consists of a single cell, with a BS, which is located at the center of the cell. The UEs are uniformly distributed in the cell. The BS and the UEs have multiple antennas, M, for the BS and K, for each UE, however, the BS has far more antennas than each of the UEs. For the sake of simplicity, K is assumed to be the same for all UEs. The focus of the simulations is uplink. In each time slot, each UE transmits a fixed number of symbols. The channel paths among the UEs are uncorrelated, and so are the individual antenna paths per UE. For each SNR, Monte Carlo simulations are performed over 10K iterations.

We simulated three major use-cases over this setup: conventional Massive MIMO (without any network coding), Massive MIMO with network layer NC and Massive MIMO with physical layer NC. We present the results for different variants of the M-QAM over these three use-cases in III-B.

$$LL_i(s_i \oplus s_{Q+i} = -1) \approx \max\left(\frac{2\widehat{s}_{\mathrm{sd,i}} - 2}{\sigma_i^2}, -\frac{2\widehat{s}_{\mathrm{sd,i}} - 2}{\sigma_i^2}\right) + \ln\left(1 + e^{-\left|\frac{4\widehat{s}_{\mathrm{sd,i}}}{\sigma_i^2}\right|}\right). \tag{30}$$

$$LL_{Q+i}(s_i \oplus s_{Q+i} = +1) \approx \max\left(\frac{2\widehat{s}_{\mathrm{sd,Q+i}} - 2}{\sigma_{Q+i}^2}, -\frac{2\widehat{s}_{\mathrm{sd,Q+i}} - 2}{\sigma_{Q+i}^2}\right) + \ln\left(1 + e^{-\left|\frac{4\widehat{s}_{\mathrm{sd,Q+i}}}{\sigma_{Q+i}^2}\right|}\right). \tag{31}$$

$$\widehat{s_i \oplus s_{Q+i}} = \begin{cases} +1, \, LL_{Q+i}(s_i \oplus s_{Q+i} = +1) \geq LL_i(s_i \oplus s_{Q+i} = -1) \\ -1, \, LL_{Q+i}(s_i \oplus s_{Q+i} = +1) < LL_i(s_i \oplus s_{Q+i} = -1) \end{cases}. \tag{32}$$

TABLE II
PNC MAPPING OF I/Q-COMPONENT OF 16-QAM, BASED ON SD SCHEME

s_i	s_{Q+i}	$s_{\mathrm{sd,i}}$	$s_{\mathrm{sd,Q+i}}$	s^i_{PNC}
1	1	2	0	-3
1	-1	0	2	3
1	3	4	-2	-1
1	-3	-2	4	1
-1	1	0	-2	3
-1	-1	-2	0	-3
-1	3	2	-4	1
-1	-3	-4	2	-1

s_i	s_{Q+i}	$s_{\mathrm{sd,i}}$	$s_{\mathrm{sd,Q+i}}$	s^i_{PNC}
3	1	4	2	-1
3	-1	2	4	1
3	3	6	0	-3
3	-3	0	6	3
-3	1	-2	-4	1
-3	-1	-4	-2	-1
-3	3	0	-6	3
-3	-3	-6	0	-3

$$\begin{aligned}
LL(s_i \oplus s_{Q+i} \ = -3) &= \ln\left[L(\widehat{s_i \oplus s_{Q+i}} = -3 | \widehat{s}_{\mathrm{sd,i}}, \widehat{s}_{\mathrm{sd,Q+i}})\right] \\
&= \ln\Big[P(\widehat{s}_{\mathrm{sd,i}}|s_{\mathrm{sd,i}} = +2)P(\widehat{s}_{\mathrm{sd,Q+i}}|s_{\mathrm{sd,Q+i}} = 0) + P(\widehat{s}_{\mathrm{sd,i}}|s_{\mathrm{sd,i}} = -2)P(\widehat{s}_{\mathrm{sd,Q+i}}|s_{\mathrm{sd,Q+i}} = 0) \\
&\quad + P(\widehat{s}_{\mathrm{sd,i}}|s_{\mathrm{sd,i}} = +6)P(\widehat{s}_{\mathrm{sd,Q+i}}|s_{\mathrm{sd,Q+i}} = 0) + P(\widehat{s}_{\mathrm{sd,i}}|s_{\mathrm{sd,i}} = -6)P(\widehat{s}_{\mathrm{sd,Q+i}}|s_{\mathrm{sd,Q+i}} = 0)\Big] \\
&= \ln\left[\frac{1}{2\pi\sqrt{\sigma_i^2\sigma_{Q+i}^2}} e^{-\frac{\widehat{s}^2_{\mathrm{sd,Q+i}}}{2\sigma_{Q+i}^2}} \left(e^{-\frac{\left(\widehat{s}_{\mathrm{sd,i}} - 2\right)^2}{2\sigma_i^2}} + e^{-\frac{\left(\widehat{s}_{\mathrm{sd,i}} + 2\right)^2}{2\sigma_i^2}} + e^{-\frac{\left(\widehat{s}_{\mathrm{sd,i}} - 6\right)^2}{2\sigma_i^2}}\right.\right. \\
&\quad \left.\left. + e^{-\frac{\left(\widehat{s}_{\mathrm{sd,i}} + 6\right)^2}{2\sigma_i^2}}\right)\right] \\
&= \ln\left[\frac{1}{2\pi\sqrt{\sigma_i^2\sigma_{Q+i}^2}} e^{-\left(\frac{\widehat{s}^2_{\mathrm{sd,Q+i}}}{2\sigma_{Q+i}^2} + \frac{\widehat{s}^2_{\mathrm{sd,i}} + 4}{2\sigma_i^2}\right)} \left(\cosh\left(\frac{2\widehat{s}_{\mathrm{sd,i}}}{\sigma_i^2}\right) + \cosh\left(\frac{6\widehat{s}_{\mathrm{sd,i}}}{\sigma_i^2}\right) e^{-\frac{16}{\sigma_i^2}}\right)\right].
\end{aligned} \tag{35}$$

$$
\begin{aligned}
LL(s_i \oplus s_{Q+i} \ = -1) &= \ln\left[L(s_i \widehat{\oplus\, s_{Q+i}} = -1|\widehat{s}_{\text{sd,i}}, \widehat{s}_{\text{sd,Q+i}})\right] \\
&= \ln\Big[P(\widehat{s}_{\text{sd,i}}|s_{\text{sd,i}} = +4)P(\widehat{s}_{\text{sd,Q+i}}|s_{\text{sd,Q+i}} = -2) + P(\widehat{s}_{\text{sd,i}}|\widehat{s}_{\text{sd,i}} = -4)P(\widehat{s}_{\text{sd,Q+i}}|s_{\text{sd,Q+i}} = +2) \\
&+ P(\widehat{s}_{\text{sd,i}}|s_{\text{sd,i}} = +4)P(\widehat{s}_{\text{sd,Q+i}}|s_{\text{sd,Q+i}} = +2) + P(\widehat{s}_{\text{sd,i}}|s_{\text{sd,i}} = -4)P(\widehat{s}_{\text{sd,Q+i}}|s_{\text{sd,Q+i}} = -2)\Big] \\
&= \ln\left[\frac{1}{2\pi\sqrt{\sigma_i^2\sigma_{Q+i}^2}}e^{-\left(\frac{\widehat{s}_{\text{sd,i}}^2+16}{2\sigma_i^2}+\frac{\widehat{s}_{\text{sd,Q+i}}^2+4}{2\sigma_{Q+i}^2}\right)}\cosh\left(\frac{4\widehat{s}_{\text{sd,i}}}{\sigma_i^2}\right)\cosh\left(\frac{2\widehat{s}_{\text{sd,Q+i}}}{\sigma_{Q+i}^2}\right)\right] .
\end{aligned} \tag{36}
$$

$$
\begin{aligned}
LL(s_i \oplus s_{Q+i} \ = +1) &= \ln\left[L(s_i \widehat{\oplus\, s_{Q+i}} = +1|\widehat{s}_{\text{sd,i}}, \widehat{s}_{\text{sd,Q+i}})\right] \\
&= \ln\Big[P(\widehat{s}_{\text{sd,i}}|s_{\text{sd,i}} = -2)P(\widehat{s}_{\text{sd,Q+i}}|s_{\text{sd,Q+i}} = +4) + P(\widehat{s}_{\text{sd,i}}|s_{\text{sd,i}} = +2)P(\widehat{s}_{\text{sd,Q+i}}|s_{\text{sd,Q+i}} = -4) \\
&+ P(\widehat{s}_{\text{sd,i}}|s_{\text{sd,i}} = +2)P(\widehat{s}_{\text{sd,Q+i}}|s_{\text{sd,Q+i}} = +4) + P(\widehat{s}_{\text{sd,i}}|s_{\text{sd,i}} = -2)P(\widehat{s}_{\text{sd,Q+i}}|s_{\text{sd,Q+i}} = -4)\Big] \\
&= \ln\left[\frac{1}{2\pi\sqrt{\sigma_i^2\sigma_{Q+i}^2}}e^{-\left(\frac{\widehat{s}_{\text{sd,Q+i}}^2+16}{2\sigma_{Q+i}^2}+\frac{\widehat{s}_{\text{sd,i}}^2+4}{2\sigma_i^2}\right)}\cosh\left(\frac{4\widehat{s}_{\text{sd,Q+i}}}{\sigma_{Q+i}^2}\right)\cosh\left(\frac{2\widehat{s}_{\text{sd,i}}}{\sigma_i^2}\right)\right] .
\end{aligned} \tag{37}
$$

$$
\begin{aligned}
LL(s_i \oplus s_{Q+i} \ = +3) &= \ln\left[L(s_i \widehat{\oplus\, s_{Q+i}} = +3|\widehat{s}_{\text{sd,i}}, \widehat{s}_{\text{sd,Q+i}})\right] \\
&= \ln\Big[P(\widehat{s}_{\text{sd,i}}|s_{\text{sd,i}} = 0)P(\widehat{s}_{\text{sd,Q+i}}|s_{\text{sd,Q+i}} = +2) + P(\widehat{s}_{\text{sd,i}}|s_{\text{sd,i}} = 0)P(\widehat{s}_{\text{sd,Q+i}}|s_{\text{sd,Q+i}} = -2) \\
&+ P(\widehat{s}_{\text{sd,i}}|s_{\text{sd,i}} = 0)P(\widehat{s}_{\text{sd,Q+i}}|s_{\text{sd,Q+i}} = +6) + P(\widehat{s}_{\text{sd,i}}|s_{\text{sd,i}} = 0)P(\widehat{s}_{\text{sd,Q+i}}|s_{\text{sd,Q+i}} = -6)\Big] \\
&= \ln\left[\frac{1}{2\pi\sqrt{\sigma_i^2\sigma_{Q+i}^2}}e^{-\left(\frac{\widehat{s}_{\text{sd,i}}}{2\sigma_i^2}+\frac{\widehat{s}_{\text{sd,Q+i}}+4}{2\sigma_{Q+i}^2}\right)}\left(\cosh\left(\frac{2\widehat{s}_{\text{sd,Q+i}}}{\sigma_{Q+i}^2}\right)+\cosh\left(\frac{6\widehat{s}_{\text{sd,Q+i}}}{\sigma_{Q+i}^2}\right)e^{-\frac{16}{\sigma_{Q+i}^2}}\right)\right] .
\end{aligned} \tag{38}
$$

TABLE III
SIMULATION PARAMETERS

Parameters	***Values***
No. antennas at relay, M	[4, 64, 120]
No. antennas per UE, K	[2, 4, 10]
No. UEs, N	[2, 16, 12]
Channel, H	i.i.d Rayleigh
SNR in dB	$0 \ldots 50$
Modulation	4-QAM, 16-QAM, 64-QAM
Packet size per UE	100 symbols
No. iterations	10^4
Channel Coding	Uncoded
Linear Detectors	ZF, MMSE

B. Performance Analysis

In the analysis, we compare the BER of the three use-cases of conventional Massive MIMO, Massive MIMO with NC and Massive MIMO with PNC. Comparing the BER of the conventional Massive MIMO to our work on Massive MIMO and PNC is necessary in order to ascertain if the former's decoding performance is sacrificed at the expense of incorporating PNC into Massive MIMO. To reiterate, ZF and MMSE were adopted without any modification in our PNC scheme, and therefore BER of the Massive MIMO and PNC is expected not to be worse than that of the conventional Massive MIMO.

In Fig. 3, we compare the BER of conventional Massive MIMO, Massive MIMO with NC and Massive MIMO with PNC, where the detection scheme is ZF, and with the following parameters: $M = 64$, $N = 16$, $K = 4$, and the modulation schemes are 4-QAM, 16-QAM, and 64-QAM. The mathematical derivations for the MAP-based PNC mapping

function for 64-QAM are included in the Appendix. The figure reveals that, irrespective of the modulation scheme, the BER of Massive MIMO and PNC was better than the conventional Massive MIMO, exceeding our expectation. This can be attributed to the fact that the ZF linear detector does not have to detect the individual transmitted symbols, rather a sum and difference of the transmitted symbols will be detected, and then, soft decoding into the PNC symbols using the MAP decoder are implemented. Looking closely at varying M-QAM across all usecases, the plots reveal relatively progressive error performance as SNR increases, which is higher for higher order dimension, e.g. 64-QAM. Although diversity gain has increased upon having huge number of antennas at the BS, so has interference and noise at the receive antennas. As interference and noise accumulate at the receive antennas, it is difficulty to correct erroneously detected symbols of a higher order modulation scheme. Hence, ZF detection may not be suitable for Massive MIMO and PNC for higher order modulations schemes such as 64-QAM, due to its inability to address noise accumulations.

Fig. 4 considers the same simulation parameters as in Fig. 3, except the linear detector is MMSE-based. Again, in this figure, the BER of Massive MIMO and PNC is lower than the BER of conventional Massive MIMO, closely aligning with the results in Fig. 3. The plots also show that as the SNR approaches 25dB, the BER of Massive MIMO and PNC for 4-QAM decreases sharply compared to Massive MIMO and PNC for 16-QAM and 64-QAM. The modulation scheme of 4-QAM appears to be the preferred transmission scheme in the lower SNRs and when throughput is small. However, 64-QAM may be the preferred modulation scheme for Massive MIMO and PNC as SNR increases. In general, if the noise variance at the receive antennas can be easily determined, then MMSE-based Massive MIMO and PNC is preferred, when the number of BS antennas is big.

The simulation setup for Fig. 5 and Fig. 6 are, respectively, the higher order antenna dimension of Fig. 3 and Fig. 4. The simulation parameters are: $M = 120$, $N = 30$, $K = 4$. Modulation 4-QAM, 16-QAM, and 64-QAM are deployed in both Fig. 5 and Fig. 6, with the former using ZF and the latter, MMSE linear detection. Again, in both figures, the BER of our Massive MIMO and PNC scheme peformed better than conventional Massive MIMO, exceeding our expectations. The plots in Fig. 5 reveal that Massive MIMO with PNC utilizing 4-QAM performs better than those with 16-QAM and 64-QAM, but requires higher SNR to achieve that performance. Again, ZF may not be the appropriate the detection scheme for the lower SNRs. Fig. 6, on the other hand, reveals that Massive MIMO and PNC with 64-QAM performs better in the higher SNRs, making it the ideal setup for higher throughput requirements.

In Fig. 7, our proposed scheme using MMSE and ZF was bench-marked against an optimal detector in ML, in MIMO system with just 4 antennas at the BS and two users, each with two antennas. Evidently, our proposed scheme with ML detector performed way better than that of the ZF and MMSE and this trend of performance will be similar for higher order dimension of antennas and the higher order of the

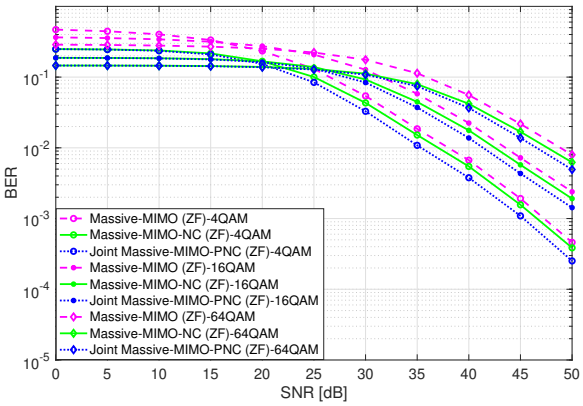

Fig. 3. Uplink BER performance comparison between i) conventional multi-user MIMO ii) multi-user MIMO with network layer NC and iii) multi-user MIMO with PNC), all using ZF detector, for M=64, N=16 and K=4.

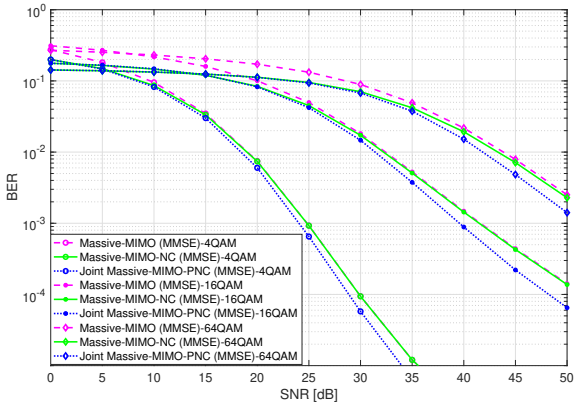

Fig. 4. Uplink BER performance comparison between i) conventional multi-user MIMO ii) multi-user MIMO with network layer NC and iii) multi-user MIMO with PNC), all using MMSE detector, for M=64, N=16 and K=4.

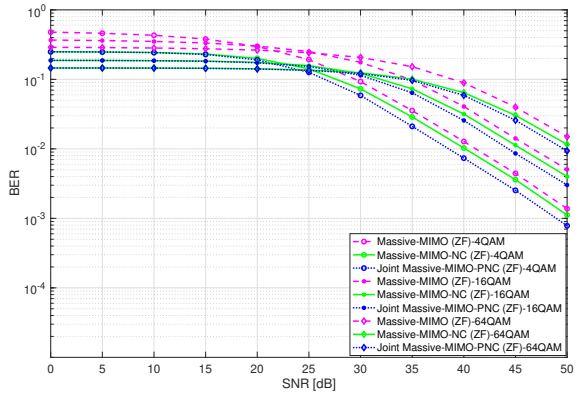

Fig. 5. Uplink BER performance comparison between i) conventional multi-user MIMO ii) multi-user MIMO with network layer NC and iii) multi-user MIMO with PNC), all using ZF detector, for M=128, N=16 and K=8.

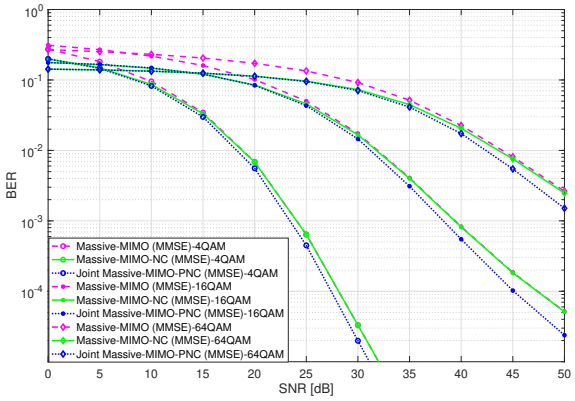

Fig. 6. Uplink BER performance comparison between i) conventional multi-user MIMO ii) multi-user MIMO with network layer NC and iii) multi-user MIMO with PNC), all using MMSE detector, for M=128, N=16 and K=8.

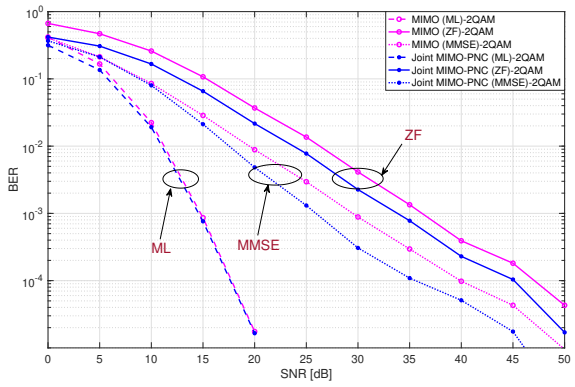

Fig. 7. Uplink BER performance comparison between i) conventional multi-user MIMO and ii) multi-user MIMO with PNC), all using ZF, MMSE detector and ML, for M=4, N=2 and K=2.

QAM. ML is not practical enough because of the exponential computational complexity as the number of antenna increases and also as the order of dimension of the QAM increases. However, the result asserts the notion that ZF and MMSE can be replaced with other higher performance sub-optimal detectors, and our proposed scheme's performance will scale accordingly.

Our proposed PNC scheme's decoding complexity lies on the product of the number of users and number antennas that each user has. The larger the cumulative number of the transmit antennas, the higher complexity in correctly estimating the PNC symbols. However, in practical systems, user devices may not be equipped with large number of antennas as opposed to the massive number of antennas at the BS. The order of dimension of the QAM also plays a role in the PNC decoding complexity. Much like having large number of antennas, the higher the order of the M-Ary QAM, the more constellation values, the more the sum and difference symbols, and the higher the complexity in decoding.

The performance of our proposed scheme can also be explained utilizing the minimum distance concept [30]. The goal is to characterize the minimum distance between two NC symbols. However, in our proposed scheme, because we

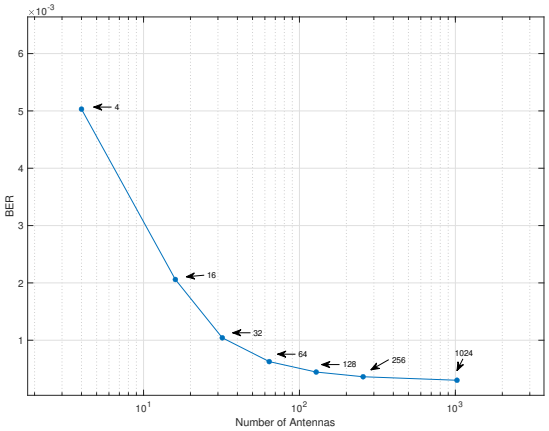

Fig. 8. BER of proposed M-MIMO PNC scheme against the number of antennas

derive the PNC symbols from the SD symbols, the minimum distance among the SD symbols is rather pertinent. Taking 4-QAM for example, the constellation values of the independent I/Q phases are $\{+1, -1\}$, leading SD symbols to be $\{2, 0, -2\}$ as shown in Table I. It is evident that the minimum distance of the SD symbols is no different than the minimum distance of the transmitted symbols. It means, rather detecting the transmitted symbols and deriving the NC symbols, if we detect the SD symbols, the decoding performance of the latter is expected not to be much worse or better than the former. However, considering Table I, for example, mapping the detected SD symbols to PNC symbol of +1, does not require that both the sum and difference are decoded correctly. If the detected sum is zero, without detecting that the difference is either +2 or -2, a +1 PNC symbol can be assumed. Similar approach goes for mapping detected SD symbols to PNC symbol of -1. This approach seems to lower the probability of error in correctly decoding the PNC symbol allowing our proposed scheme to perform slightly better than the conventional M-MIMO, where the decision region is definite in detecting the individual transmitted symbols.

Our proposed scheme also benefits from the law of large numbers as much as underlying Massive MIMO systems. In Fig. 8, we plotted the BER of our proposed scheme against variation of number of antennas, whilst fixing the SNR and the modulation scheme. In the figure, one can notice that as the number of antennas increases, the BER of our proposed scheme decreases exponentially till a point where the channel starts to harden, where the noise starts to average out causing the impact of fading to diminish, leading to lower probability of error.

It is also evident from the results that the performance was presented with respect to DL. Our proposed scheme is applicable at the interference point, which is the UL. This is where PNC is performed by the BS. In essence, the BS receives interfered symbols, apply our proposed scheme and then generate the PNC symbols. In DL, the BS transmits the derived PNC symbols to respective UEs in a way similar to how conventional Massive MIMO operates in DL. Therefore,

the performance evaluation in DL is similar to those for the conventional Massive MIMO in the literature.

IV. Conclusions

A practical approach for deploying PNC in M-QAM Massive MIMO systems was proposed in this paper. A new PNC mapping scheme based on clusters of estimated SD of the transmitted symbols from user pairs was developed to enable using PNC in massive MIMO systems. Utilizing existing linear detectors, such as ZF and MMSE and using an SD linearly transformed channel matrix, the SD symbols are detected. Employing MAP soft decoding, we mapped the detected SD symbols to the PNC symbols. The simulation results reveal that, using existing MIMO detection schemes, our proposed scheme achieves twice the spectral efficiency of conventional Massive MIMO. The BER of our scheme was slightly better than the conventional Massive MIMO, indicating that our proposed PNC scheme can be deployed without sacrificing the BER of the conventional Massive MIMO. Furthermore, the results also revealed that for lower throughput and at low SNR, 4-QAM appears to be the preferred modulation scheme, whereas 64-QAM or higher is the preferred scheme in higher SNR, satisfying a higher throughput requirement. Further research is however needed in order to make this a reality in deployed systems. For example, research in integrating channel coding is needed to improve on the error performance and get the proposed scheme closer to real systems. Research in users transmitting with different QAM modulation schemes is also needed to get the proposed scheme close to real systems. Also, dealing with asynchronous transmission by multiple sources with our proposed scheme as the underlying PNC system requires further research.

V. Acknowledgement

This work has been funded by the European Union Horizon 2020, RISE 2018 scheme (H2020-MSCA-RISE-2018) under the Marie Skłodowska-Curie grant agreement No. 823903 (RECENT).

VI. Appendix A

A. Specialization of the PNC Mapping for 64-QAM

When the transmitting nodes are utilizing 64-QAM modulation scheme, Table IV shows the corresponding mapped PNC symbols, $\boldsymbol{s}_{\text{PNC}}^{i}$, and the expected SD symbols, $\boldsymbol{s}_{\text{sd,i}}$ and $\boldsymbol{s}_{\text{sd,Q+i}}$, of the transmitted symbols, $\boldsymbol{s}_i$ and $\boldsymbol{s}_{Q+i}$. The log-likelihood of PNC symbols +1, -1, +3, -3, +5, -5, +7 and -7, given that a cluster has $\widehat{s}_{\text{sd,i}}$ and $\widehat{s}_{\text{sd,Q+i}}$ estimated SD symbols, are expressed, respectively, as in (39)-(46).

TABLE IV
PNC Mapping Of I/Q-Component Of 64-QAM, Based On SD Scheme

$\boldsymbol{s}_i$	$\boldsymbol{s}_{Q+i}$	$\boldsymbol{s}_{\text{sd,i}}$	$\boldsymbol{s}_{\text{sd,Q+i}}$	$\boldsymbol{s}_{\text{PNC}}^{i}$	$\boldsymbol{s}_i$	$\boldsymbol{s}_{Q+i}$	$\boldsymbol{s}_{\text{sd,i}}$	$\boldsymbol{s}_{\text{sd,Q+i}}$	$\boldsymbol{s}_{\text{PNC}}^{i}$
1	1	2	0	1	5	1	6	4	5
1	-1	0	2	-1	5	-1	4	6	-5
1	3	4	-2	3	5	3	8	2	7
1	-3	-2	4	-3	5	-3	2	8	-7
1	5	6	-4	5	5	5	10	0	1
1	-5	-4	6	-5	5	-5	0	10	-1
1	7	8	-6	7	5	7	12	-2	3
1	-7	-6	8	-7	5	-7	-2	12	-3
-1	1	0	-2	-1	-5	1	-4	-6	-5
-1	-1	-2	0	1	-5	-1	-6	-4	5
-1	3	2	-4	-3	-5	3	-2	-8	-7
-1	-3	-4	2	3	-5	-3	-8	-2	7
-1	5	4	-6	-5	-5	5	0	-10	-1
-1	-5	-6	4	5	-5	-5	-10	0	1
-1	7	6	-8	-7	-5	7	2	-12	-3
-1	-7	-8	6	7	-5	-7	-12	2	3
3	1	4	2	3	7	1	8	6	7
3	-1	2	4	-3	7	-1	6	8	-7
3	3	6	0	1	7	3	10	4	5
3	-3	0	6	-1	7	-3	4	10	-5
3	5	8	-2	7	7	5	12	2	3
3	-5	-2	8	-7	7	-5	2	12	-3
3	7	10	-4	5	7	7	14	0	1
3	-7	-4	10	-5	7	-7	0	14	-1
-3	1	-2	-4	-3	-7	1	-6	-8	-7
-3	-1	-4	-2	3	-7	-1	-8	-6	7
-3	3	0	-6	-1	-7	3	-4	-10	-5
-3	-3	-6	0	1	-7	-3	-10	-4	5
-3	5	2	-8	-7	-7	5	-2	-12	-3
-3	-5	-8	2	7	-7	-5	-12	-2	3
-3	7	4	-10	-5	-7	7	0	-14	-1
-3	-7	-10	4	5	-7	-7	-14	0	1

$$
\begin{aligned}
LL(s_i \oplus s_{Q+i} \ = +1) &= \ln\left[L(s_i \widehat{\oplus s_{Q+i}} = +1|\widehat{s}_{\mathrm{sd,i}}, \widehat{s}_{\mathrm{sd,Q+i}})\right] \\
&= \ln\Big[P(\widehat{s}_{\mathrm{sd,i}}|s_{\mathrm{sd,i}} = +2)P(\widehat{s}_{\mathrm{sd,Q+i}}|s_{\mathrm{sd,Q+i}} = 0) + P(\widehat{s}_{\mathrm{sd,i}}|s_{\mathrm{sd,i}} = -2)P(\widehat{s}_{\mathrm{sd,Q+i}}|s_{\mathrm{sd,Q+i}} = 0) \\
&+ P(\widehat{s}_{\mathrm{sd,i}}|s_{\mathrm{sd,i}} = +6)P(\widehat{s}_{\mathrm{sd,Q+i}}|s_{\mathrm{sd,Q+i}} = 0) + P(\widehat{s}_{\mathrm{sd,i}}|s_{\mathrm{sd,i}} = -6)P(\widehat{s}_{\mathrm{sd,Q+i}}|s_{\mathrm{sd,Q+i}} = 0) \\
&+ P(\widehat{s}_{\mathrm{sd,i}}|s_{\mathrm{sd,i}} = +10)P(\widehat{s}_{\mathrm{sd,Q+i}}|s_{\mathrm{sd,Q+i}} = 0) + P(\widehat{s}_{\mathrm{sd,i}}|s_{\mathrm{sd,i}} = -10)P(\widehat{s}_{\mathrm{sd,Q+i}}|s_{\mathrm{sd,Q+i}} = 0) \\
&+ P(\widehat{s}_{\mathrm{sd,i}}|s_{\mathrm{sd,i}} = +14)P(\widehat{s}_{\mathrm{sd,Q+i}}|s_{\mathrm{sd,Q+i}} = 0) + P(\widehat{s}_{\mathrm{sd,i}}|s_{\mathrm{sd,i}} = -14)P(\widehat{s}_{\mathrm{sd,Q+i}}|s_{\mathrm{sd,Q+i}} = 0)\Big] \\
&= \ln\left[\frac{1}{2\pi\sqrt{\sigma_i^2\sigma_{Q+i}^2}} e^{-\left(\frac{\widehat{s}_{\mathrm{sd,Q+i}}^2}{2\sigma_{Q+i}^2} + \frac{\widehat{s}_{\mathrm{sd,i}}^2 + 4}{2\sigma_i^2}\right)} \left(\cosh\left(\frac{2\widehat{s}_{\mathrm{sd,i}}}{\sigma_i^2}\right) + \cosh\left(\frac{6\widehat{s}_{\mathrm{sd,i}}}{\sigma_i^2}\right) e^{-\frac{16}{\sigma_i^2}}\right.\right. \\
&\left.\left. + \cosh\left(\frac{10\widehat{s}_{\mathrm{sd,i}}}{\sigma_i^2}\right) e^{-\frac{48}{\sigma_i^2}} + \cosh\left(\frac{14\widehat{s}_{\mathrm{sd,i}}}{\sigma_i^2}\right) e^{-\frac{96}{\sigma_i^2}}\right)\right], \qquad (39)
\end{aligned}
$$

$$
\begin{aligned}
LL(s_i \oplus s_{Q+i} \ = -1) &= \ln\left[L(s_i \widehat{\oplus s_{Q+i}} = -1|\widehat{s}_{\mathrm{sd,i}}, \widehat{s}_{\mathrm{sd,Q+i}})\right] \\
&= \ln\Big[P(\widehat{s}_{\mathrm{sd,i}}|s_{\mathrm{sd,i}} = 0)P(\widehat{s}_{\mathrm{sd,Q+i}}|s_{\mathrm{sd,Q+i}} = +2) + P(\widehat{s}_{\mathrm{sd,i}}|s_{\mathrm{sd,i}} = 0)P(\widehat{s}_{\mathrm{sd,Q+i}}|s_{\mathrm{sd,Q+i}} = -2) \\
&+ P(\widehat{s}_{\mathrm{sd,i}}|s_{\mathrm{sd,i}} = 0)P(\widehat{s}_{\mathrm{sd,Q+i}}|s_{\mathrm{sd,Q+i}} = +6) + P(\widehat{s}_{\mathrm{sd,i}}|s_{\mathrm{sd,i}} = 0)P(\widehat{s}_{\mathrm{sd,Q+i}}|s_{\mathrm{sd,Q+i}} = -6) \\
&+ P(\widehat{s}_{\mathrm{sd,i}}|s_{\mathrm{sd,i}} = 0)P(\widehat{s}_{\mathrm{sd,Q+i}}|s_{\mathrm{sd,Q+i}} = +10) + P(\widehat{s}_{\mathrm{sd,i}}|s_{\mathrm{sd,i}} = 0)P(\widehat{s}_{\mathrm{sd,Q+i}}|s_{\mathrm{sd,Q+i}} = -10) \\
&+ P(\widehat{s}_{\mathrm{sd,i}}|s_{\mathrm{sd,i}} = 0)P(\widehat{s}_{\mathrm{sd,Q+i}}|s_{\mathrm{sd,Q+i}} = +14) + P(\widehat{s}_{\mathrm{sd,i}}|s_{\mathrm{sd,i}} = 0)P(\widehat{s}_{\mathrm{sd,Q+i}}|s_{\mathrm{sd,Q+i}} = -14)\Big] \\
&= \ln\left[\frac{1}{2\pi\sqrt{\sigma_i^2\sigma_{Q+i}^2}} e^{-\left(\frac{\widehat{s}_{\mathrm{sd,i}}^2}{2\sigma_i^2} + \frac{\widehat{s}_{\mathrm{sd,Q+i}}^2 + 4}{2\sigma_{Q+i}^2}\right)} \left(\cosh\left(\frac{2\widehat{s}_{\mathrm{sd,Q+i}}}{\sigma_{Q+i}^2}\right) + \cosh\left(\frac{6\widehat{s}_{\mathrm{sd,Q+i}}}{\sigma_{Q+i}^2}\right) e^{-\frac{16}{\sigma_{Q+i}^2}}\right.\right. \\
&\left.\left. + \cosh\left(\frac{10\widehat{s}_{\mathrm{sd,Q+i}}}{\sigma_{Q+i}^2}\right) e^{-\frac{48}{\sigma_{Q+i}^2}} + \cosh\left(\frac{14\widehat{s}_{\mathrm{sd,Q+i}}}{\sigma_{Q+i}^2}\right) e^{-\frac{96}{\sigma_{Q+i}^2}}\right)\right], \qquad (40)
\end{aligned}
$$

$$
\begin{aligned}
LL(s_i \oplus s_{Q+i} \ = +3) &= \ln\left[L(s_i \widehat{\oplus s_{Q+i}} = +3|\widehat{s}_{\mathrm{sd,i}}, \widehat{s}_{\mathrm{sd,Q+i}})\right] \\
&= \ln\Big[P(\widehat{s}_{\mathrm{sd,Q+i}}|s_{\mathrm{sd,i}} = +4)P(\widehat{s}_{\mathrm{sd,Q+i}}|s_{\mathrm{sd,Q+i}} = -2) + P(\widehat{s}_{\mathrm{sd,Q+i}}|s_{\mathrm{sd,i}} = -4)P(\widehat{s}_{\mathrm{sd,Q+i}}|s_{\mathrm{sd,Q+i}} = +2) \\
&+ P(\widehat{s}_{\mathrm{sd,Q+i}}|s_{\mathrm{sd,i}} = +4)P(\widehat{s}_{\mathrm{sd,Q+i}}|s_{\mathrm{sd,Q+i}} = +2) + P(\widehat{s}_{\mathrm{sd,Q+i}}|s_{\mathrm{sd,i}} = -4)P(\widehat{s}_{\mathrm{sd,Q+i}}|s_{\mathrm{sd,Q+i}} = -2) \\
&+ P(\widehat{s}_{\mathrm{sd,Q+i}}|s_{\mathrm{sd,i}} = +12)P(\widehat{s}_{\mathrm{sd,Q+i}}|s_{\mathrm{sd,Q+i}} = -2) + P(\widehat{s}_{\mathrm{sd,Q+i}}|s_{\mathrm{sd,i}} = -12)P(\widehat{s}_{\mathrm{sd,Q+i}}|s_{\mathrm{sd,Q+i}} = +2) \\
&+ P(\widehat{s}_{\mathrm{sd,Q+i}}|s_{\mathrm{sd,i}} = +12)P(\widehat{s}_{\mathrm{sd,Q+i}}|s_{\mathrm{sd,Q+i}} = +2) + P(\widehat{s}_{\mathrm{sd,Q+i}}|s_{\mathrm{sd,i}} = -12)P(\widehat{s}_{\mathrm{sd,Q+i}}|s_{\mathrm{sd,Q+i}} = -2)\Big] \\
&= \ln\left[\frac{1}{2\pi\sqrt{\sigma_i^2\sigma_{Q+i}^2}} e^{-\left(\frac{\widehat{s}_{\mathrm{sd,Q+i}}^2 + 4}{2\sigma_{Q+i}^2} + \frac{\widehat{s}_{\mathrm{sd,i}}^2 + 16}{2\sigma_i^2}\right)} \cosh\left(\frac{2\widehat{s}_{\mathrm{sd,Q+i}}}{\sigma_{Q+i}^2}\right) \left(\cosh\left(\frac{4\widehat{s}_{\mathrm{sd,i}}}{\sigma_i^2}\right)\right.\right. \\
&\left.\left. + \cosh\left(\frac{14\widehat{s}_{\mathrm{sd,i}}}{\sigma_i^2}\right) e^{-\frac{128}{\sigma_i^2}}\right)\right], \qquad (41)
\end{aligned}
$$

$$
\begin{aligned}
LL(s_i \oplus s_{Q+i} \ = -3) &= \ln\left[L(\widehat{s_i \oplus s_{Q+i}} = -3|\widehat{s}_{\mathrm{sd,i}}, \widehat{s}_{\mathrm{sd,Q+i}})\right] \\
&= \ln\Big[P(\widehat{s}_{\mathrm{sd,i}}|s_{\mathrm{sd,i}} = -2)P(\widehat{s}_{\mathrm{sd,Q+i}}|s_{\mathrm{sd,Q+i}} = +4) + P(\widehat{s}_{\mathrm{sd,i}}|s_{\mathrm{sd,i}} = +2)P(\widehat{s}_{\mathrm{sd,Q+i}}|s_{\mathrm{sd,Q+i}} = -4) \\
&+ P(\widehat{s}_{\mathrm{sd,i}}|s_{\mathrm{sd,i}} = +2)P(\widehat{s}_{\mathrm{sd,Q+i}}|s_{\mathrm{sd,Q+i}} = +4) + P(\widehat{s}_{\mathrm{sd,i}}|s_{\mathrm{sd,i}} = -2)P(\widehat{s}_{\mathrm{sd,Q+i}}|s_{\mathrm{sd,Q+i}} = -4) \\
&+ P(\widehat{s}_{\mathrm{sd,i}}|s_{\mathrm{sd,i}} = -2)P(\widehat{s}_{\mathrm{sd,Q+i}}|s_{\mathrm{sd,Q+i}} = +12) + P(\widehat{s}_{\mathrm{sd,i}}|s_{\mathrm{sd,i}} = +2)P(\widehat{s}_{\mathrm{sd,Q+i}}|s_{\mathrm{sd,Q+i}} = -12) \\
&+ P(\widehat{s}_{\mathrm{sd,i}}|s_{\mathrm{sd,i}} = +2)P(\widehat{s}_{\mathrm{sd,Q+i}}|s_{\mathrm{sd,Q+i}} = +12) + P(\widehat{s}_{\mathrm{sd,i}}|s_{\mathrm{sd,i}} = -2)P(\widehat{s}_{\mathrm{sd,Q+i}}|s_{\mathrm{sd,Q+i}} = -12)\Big] \\
&= \ln\left[\frac{1}{2\pi\sqrt{\sigma_i^2\sigma_{Q+i}^2}}e^{-\left(\frac{\widehat{s}_{\mathrm{sd,i}}^2+4}{2\sigma_i^2}+\frac{\widehat{s}_{\mathrm{sd,Q+i}}^2+16}{2\sigma_{Q+i}^2}\right)}\cosh\left(\frac{2\widehat{s}_{\mathrm{sd,i}}}{\sigma_i^2}\right)\left(\cosh\left(\frac{4\widehat{s}_{\mathrm{sd,Q+i}}}{\sigma_{Q+i}^2}\right)\right.\right. \\
&\left.\left.+\cosh\left(\frac{14\widehat{s}_{\mathrm{sd,Q+i}}}{\sigma_{Q+i}^2}\right)e^{-\frac{128}{\sigma_{Q+i}^2}}\right)\right], \qquad (42)
\end{aligned}
$$

$$
\begin{aligned}
LL(s_i \oplus s_{Q+i} \ = +5) &= \ln\left[L(\widehat{s_i \oplus s_{Q+i}} = +5|\widehat{s}_{\mathrm{sd,i}}, \widehat{s}_{\mathrm{sd,Q+i}})\right] \\
&= \ln\Big[P(\widehat{s}_{\mathrm{sd,i}}|s_{\mathrm{sd,i}} = +6)P(\widehat{s}_{\mathrm{sd,Q+i}}|s_{\mathrm{sd,Q+i}} = -4) + P(\widehat{s}_{\mathrm{sd,i}}|s_{\mathrm{sd,i}} = -6)P(\widehat{s}_{\mathrm{sd,Q+i}}|s_{\mathrm{sd,Q+i}} = +4) \\
&+ P(\widehat{s}_{\mathrm{sd,i}}|s_{\mathrm{sd,i}} = +10)P(\widehat{s}_{\mathrm{sd,Q+i}}|s_{\mathrm{sd,Q+i}} = -4) + P(\widehat{s}_{\mathrm{sd,i}}|s_{\mathrm{sd,i}} = -10)P(\widehat{s}_{\mathrm{sd,Q+i}}|s_{\mathrm{sd,Q+i}} = +4) \\
&+ P(\widehat{s}_{\mathrm{sd,i}}|s_{\mathrm{sd,i}} = +6)P(\widehat{s}_{\mathrm{sd,Q+i}}|s_{\mathrm{sd,Q+i}} = +4) + P(\widehat{s}_{\mathrm{sd,i}}|s_{\mathrm{sd,i}} = -6)P(\widehat{s}_{\mathrm{sd,Q+i}}|s_{\mathrm{sd,Q+i}} = -4) \\
&+ P(\widehat{s}_{\mathrm{sd,i}}|s_{\mathrm{sd,i}} = +10)P(\widehat{s}_{\mathrm{sd,Q+i}}|s_{\mathrm{sd,Q+i}} = +4) + P(\widehat{s}_{\mathrm{sd,i}}|s_{\mathrm{sd,i}} = -10)P(\widehat{s}_{\mathrm{sd,Q+i}}|s_{\mathrm{sd,Q+i}} = -4)\Big] \\
&= \ln\left[\frac{1}{2\pi\sqrt{\sigma_i^2\sigma_{Q+i}^2}}e^{-\left(\frac{\widehat{s}_{\mathrm{sd,Q+i}}^2+16}{2\sigma_{Q+i}^2}+\frac{\widehat{s}_{\mathrm{sd,i}}^2+36}{2\sigma_i^2}\right)}\cosh\left(\frac{2\widehat{s}_{\mathrm{sd,Q+i}}}{\sigma_{Q+i}^2}\right)\left(\cosh\left(\frac{6\widehat{s}_{\mathrm{sd,i}}}{\sigma_i^2}\right)\right.\right. \\
&\left.\left.+\cosh\left(\frac{10\widehat{s}_{\mathrm{sd,i}}}{\sigma_i^2}\right)e^{-\frac{32}{\sigma_i^2}}\right)\right], \qquad (43)
\end{aligned}
$$

$$
\begin{aligned}
LL(s_i \oplus s_{Q+i} \ = -5) &= \ln\left[L(\widehat{s_i \oplus s_{Q+i}} = -5|\widehat{s}_{\mathrm{sd,i}}, \widehat{s}_{\mathrm{sd,Q+i}})\right] \\
&= \ln\Big[P(\widehat{s}_{\mathrm{sd,i}}|s_{\mathrm{sd,i}} = -4)P(\widehat{s}_{\mathrm{sd,Q+i}}|s_{\mathrm{sd,Q+i}} = +6) + P(\widehat{s}_{\mathrm{sd,i}}|s_{\mathrm{sd,i}} = +4)P(\widehat{s}_{\mathrm{sd,Q+i}}|s_{\mathrm{sd,Q+i}} = -6) \\
&+ P(\widehat{s}_{\mathrm{sd,i}}|s_{\mathrm{sd,i}} = -4)P(\widehat{s}_{\mathrm{sd,Q+i}}|s_{\mathrm{sd,Q+i}} = +10) + P(\widehat{s}_{\mathrm{sd,i}}|s_{\mathrm{sd,i}} = +4)P(\widehat{s}_{\mathrm{sd,Q+i}}|s_{\mathrm{sd,Q+i}} = -10) \\
&+ P(\widehat{s}_{\mathrm{sd,i}}|s_{\mathrm{sd,i}} = +4)P(\widehat{s}_{\mathrm{sd,Q+i}}|s_{\mathrm{sd,Q+i}} = +6) + P(\widehat{s}_{\mathrm{sd,i}}|s_{\mathrm{sd,i}} = -4)P(\widehat{s}_{\mathrm{sd,Q+i}}|s_{\mathrm{sd,Q+i}} = -6) \\
&+ P(\widehat{s}_{\mathrm{sd,i}}|s_{\mathrm{sd,i}} = +4)P(\widehat{s}_{\mathrm{sd,Q+i}}|s_{\mathrm{sd,Q+i}} = +10) + P(\widehat{s}_{\mathrm{sd,i}}|s_{\mathrm{sd,i}} = -4)P(\widehat{s}_{\mathrm{sd,Q+i}}|s_{\mathrm{sd,Q+i}} = -10)\Big] \\
&= \ln\left[\frac{1}{2\pi\sqrt{\sigma_i^2\sigma_{Q+i}^2}}e^{-\left(\frac{\widehat{s}_{\mathrm{sd,i}}^2+16}{2\sigma_i^2}+\frac{\widehat{s}_{\mathrm{sd,Q+i}}^2+36}{2\sigma_{Q+i}^2}\right)}\cosh\left(\frac{2\widehat{s}_{\mathrm{sd,i}}}{\sigma_i^2}\right)\left(\cosh\left(\frac{6\widehat{s}_{\mathrm{sd,Q+i}}}{\sigma_{Q+i}^2}\right)\right.\right. \\
&\left.\left.+\cosh\left(\frac{10\widehat{s}_{\mathrm{sd,Q+i}}}{\sigma_{Q+i}^2}\right)e^{-\frac{32}{\sigma_{Q+i}^2}}\right)\right], \qquad (44)
\end{aligned}
$$

$$
\begin{aligned}
LL(s_i \oplus s_{Q+i} \ = +7) &= \ln\left[L(s_i \widehat{\oplus\, s_{Q+i}} = +7|\widehat{s}_{\mathrm{sd,i}}, \widehat{s}_{\mathrm{sd,Q+i}})\right] \\
&= \ln\Big[P(\widehat{s}_{\mathrm{sd,i}}|s_{\mathrm{sd,i}} = +8)P(\widehat{s}_{\mathrm{sd,Q+i}}|s_{\mathrm{sd,Q+i}} = -6) + P(\widehat{s}_{\mathrm{sd,i}}|s_{\mathrm{sd,i}} = -8)P(\widehat{s}_{\mathrm{sd,Q+i}}|s_{\mathrm{sd,Q+i}} = +6) \\
&+ P(\widehat{s}_{\mathrm{sd,i}}|s_{\mathrm{sd,i}} = +8)P(\widehat{s}_{\mathrm{sd,Q+i}}|s_{\mathrm{sd,Q+i}} = -2) + P(\widehat{s}_{\mathrm{sd,i}}|s_{\mathrm{sd,i}} = -8)P(\widehat{s}_{\mathrm{sd,Q+i}}|s_{\mathrm{sd,Q+i}} = +2) \\
&+ P(\widehat{s}_{\mathrm{sd,i}}|s_{\mathrm{sd,i}} = +8)P(\widehat{s}_{\mathrm{sd,Q+i}}|s_{\mathrm{sd,Q+i}} = +2) + P(\widehat{s}_{\mathrm{sd,i}}|s_{\mathrm{sd,i}} = -8)P(\widehat{s}_{\mathrm{sd,Q+i}}|s_{\mathrm{sd,Q+i}} = -2) \\
&+ P(\widehat{s}_{\mathrm{sd,i}}|s_{\mathrm{sd,i}} = +8)P(\widehat{s}_{\mathrm{sd,Q+i}}|s_{\mathrm{sd,Q+i}} = +6) + P(\widehat{s}_{\mathrm{sd,i}}|s_{\mathrm{sd,i}} = -8)P(\widehat{s}_{\mathrm{sd,Q+i}}|s_{\mathrm{sd,Q+i}} = -6)\Big] \\
&= \ln\left[\frac{1}{2\pi\sqrt{\sigma_i^2\sigma_{Q+i}^2}}e^{-\left(\frac{\widehat{s}_{\mathrm{sd,i}}^2+64}{2\sigma_i^2}+\frac{\widehat{s}_{\mathrm{sd,Q+i}}^2+4}{2\sigma_{Q+i}^2}\right)}\cosh\left(\frac{4\widehat{s}_{\mathrm{sd,i}}}{\sigma_i^2}\right)\left(\cosh\left(\frac{2\widehat{s}_{\mathrm{sd,Q+i}}}{\sigma_{Q+i}^2}\right)\right.\right. \\
&\left.\left.+\cosh\left(\frac{6\widehat{s}_{\mathrm{sd,Q+i}}}{\sigma_{Q+i}^2}\right)e^{-\frac{32}{\sigma_{Q+i}^2}}\right)\right], \qquad (45)
\end{aligned}
$$

$$
\begin{aligned}
LL(s_i \oplus s_{Q+i} \ = -7) &= \ln\left[L(s_i \widehat{\oplus\, s_{Q+i}} = -7|\widehat{s}_{\mathrm{sd,i}}, \widehat{s}_{\mathrm{sd,Q+i}})\right] \\
&= \ln\Big[P(\widehat{s}_{\mathrm{sd,i}}|\widehat{s}_{\mathrm{sd,i}} = -6)P(\widehat{s}_{\mathrm{sd,Q+i}}|s_{\mathrm{sd,Q+i}} = +8) + P(\widehat{s}_{\mathrm{sd,i}}|s_{\mathrm{sd,i}} = +6)P(\widehat{s}_{\mathrm{sd,Q+i}}|s_{\mathrm{sd,Q+i}} = -8) \\
&+ P(r\widehat{s}_{\mathrm{sd,i}}|s_{\mathrm{sd,i}} = -2)P(\widehat{s}_{\mathrm{sd,Q+i}}|s_{\mathrm{sd,Q+i}} = +8) + P(\widehat{s}_{\mathrm{sd,i}}|s_{\mathrm{sd,i}} = +2)P(\widehat{s}_{\mathrm{sd,Q+i}}|s_{\mathrm{sd,Q+i}} = -8) \\
&+ P(\widehat{s}_{\mathrm{sd,i}}|s_{\mathrm{sd,i}} = +2)P(\widehat{s}_{\mathrm{sd,Q+i}}|s_{\mathrm{sd,Q+i}} = +8) + P(\widehat{s}_{\mathrm{sd,i}}|s_{\mathrm{sd,i}} = -2)P(\widehat{s}_{\mathrm{sd,Q+i}}|s_{\mathrm{sd,Q+i}} = -8) \\
&+ P(\widehat{s}_{\mathrm{sd,i}}|s_{\mathrm{sd,i}} = +6)P(\widehat{s}_{\mathrm{sd,Q+i}}|s_{\mathrm{sd,Q+i}} = +8) + P(\widehat{s}_{\mathrm{sd,i}}|s_{\mathrm{sd,i}} = -6)P(\widehat{s}_{\mathrm{sd,Q+i}}|s_{\mathrm{sd,Q+i}} = -8)\Big] \\
&= \ln\left[\frac{1}{2\pi\sqrt{\sigma_i^2\sigma_{Q+i}^2}}e^{-\left(\frac{\widehat{s}_{\mathrm{sd,Q+i}}^2+64}{2\sigma_{Q+i}^2}+\frac{\widehat{s}_{\mathrm{sd,i}}^2+4}{2\sigma_i^2}\right)}\cosh\left(\frac{4\widehat{s}_{\mathrm{sd,Q+i}}}{\sigma_{Q+i}^2}\right)\left(\cosh\left(\frac{2\widehat{s}_{\mathrm{sd,i}}}{\sigma_i^2}\right)\right.\right. \\
&\left.\left.+\cosh\left(\frac{6\widehat{s}_{\mathrm{sd,i}}}{\sigma_i^2}\right)e^{-\frac{32}{\sigma_i^2}}\right)\right]. \qquad (46)
\end{aligned}
$$

REFERENCES

[1] G. Fodor, N. Rajatheva, W. Zirwas, L. Thiele, M. Kurras, K. Guo, A. Tolli, J. H. Sorensen, E. Carvalho, "An Overview of Massive MIMO Technology Components in METIS," IEEE Commun. Mag. Vol. 6, pp. 155 - 161, June 2017.

[2] E. G. Larrson, O. Edfors, F. Tufvesson, T. L. Marzetta, "Massive MIMO for Next Generation Wireless Systems," IEEE Commun. Mag. Vol. 52, No. 2, pp. 186-195, Feb. 2014.

[3] S. A. Busari, K. M. S. Huq, S. Mumtaz, L. Dai, and J. Rodriguez, "Millimeter-Wave Massive MIMO Communication for Future Wireless Systems: A Survey," IEEE Commun. Surveys and Tuts, vol. 20, no. 2, pp. 836-869, 2nd Quart. 2018.

[4] A. Ghosh, "5G New Radio (NR) : Physical Layer Overview and Performance," IEEE Commun. Theory Workshop, May 2018, Nokia Bell Labs.

[5] S. Yang, and L. Hanzo, "Fifty years of MIMO detection: The road to large-scale MIMOs," IEEE Commun. Surveys and Tuts, vol. 17, no. 4, pp. 1941-1988, 4th Quart. 2015.

[6] R. Koetter and M. Medard "An algebraic approach to network coding" IEEE/ACM Trans. Networking, vol. 11, no. 5, pp. 782-795, Oct. 2003.

[7] S. Zhang, S. C. Liew, and P. P. Lam,"Physical layer network coding," in Proc. of the 12th Ann. Int. Conf. on Mobile Com. and Net, MOBICOM 2006, Los Angeles, CA, USA, Sept. 2006, pp. 358-365.

[8] L. Sanguinetti, E. Bjornson, and J. Hoydis, "Towards Massive MIMO 2.0: Understanding spatial correlation, interference suppression, and pilot contamination," arXiv e-prints, p. arXiv:1904.03406, Apr 2019.

[9] S. Zhang, S.C. Liew, "Physical Layer Network Coding with Multiple Antennas," IEEE Wireless Commun. and Net. Conf., 1-6, Jan. 2010.

[10] D. H. Vu, X. N. Tran, "Physical network coding for bidirectional relay MIMO-SDM system," in Proc. Int. Conf. on Advanced Techno. for Commun., 141-146, 2013.

[11] L. Shi, T. Yang, K. Cai, P. Chen and T. Guo, "On MIMO Linear Physical-Layer Network Coding: Full-Rate Full-Diversity Design and Optimization," in IEEE Transactions on Wireless Communications, vol. 17, no. 5, pp. 3498-3511, May 2018.

[12] T. Yang, X. Yuan, L. Ping, I.B. Collings and J. Yuan, "Eigen-Direction Alignment Aided Physical Layer Network Coding for MIMO Two-Way Relay Channels," in Proc. of the IEEE Int. Symp. on Information Theory (ISIT), SaintPetersburg, Russia, pp. 2253-2257, July 2011.

[13] T. Yang, X. Yuan, L. Ping, I. B. Collings, and J. Yuan, "A new physical-layer network coding scheme with eigen-direction alignment precoding for MIMO two-way relaying," IEEE Trans. Commun., vol. 61, no. 3, pp. 973-986, Mar. 2013.

[14] P. Chen, Z. Xie, Y. Fang, Z. Chen, S. Mumtaz and J. J. P. C. Rodrigues, "Physical-Layer Network Coding: An Efficient Technique for Wireless Communications," in IEEE Network, vol. 34, no. 2, pp. 270-276, March/April 2020.

[15] D. G. M. Mitchell, M. Lentmaier and D. J. Costello, "Spatially Coupled LDPC Codes Constructed From Protographs," in IEEE Transactions on Information Theory, vol. 61, no. 9, pp. 4866-4889, Sept. 2015.

[16] Y. Fang, P. Chen, G. Cai, F. C. M. Lau, S. C. Liew and G. Han, "Outage-Limit-Approaching Channel Coding for Future Wireless Communications: Root-Protograph Low-Density Parity-Check Codes," in IEEE Vehicular Technology Magazine, vol. 14, no. 2, pp. 85-93, June 2019.

[17] Z. Ding, I. Krikidis, J. Thompson, and K. K. Leung, "Physical layer

network coding and precoding for the two-way relay channel in cellular systems," IEEE Trans. Signal Process., vol. 59, no. 2, pp. 696-712, Feb. 2011.

[18] S. Liew, S. Zhang, L. Lu, "Physical-layer network coding: Tutorial survey and beyond," Phys. Commun., vol. 6, no. 1, pp. 4-42, 2013.

[19] M. Huang, J. Yuan, and T. Yang, "Error probability of physical-layer network coding in multiple-antenna two-way relay channel," in Proc. IEEE Global Communications Conference (GLOBECOM), Dec. 2012, California.

[20] M. Huang, and J. Yuan, "Physical-layer network coding with Alamouti scheme for the TWRC with linear decoder," in Proc. Australian Communications Theory Workshop (AusCTW), Feb. 2014, Sydney.

[21] M. Huang, and J. Yuan, "Error Performance of Physical-Layer Network Coding in Multiple-Antenna TWRC," IEEE Trans Vehicular Tech., vol. 63, pp. 3750 - 3761, Feb 2014.

[22] S. Zhang, Q. F. Zhou, C. Kai, W. Zhang, "Full Diversity Physical-Layer Network Coding in Two-Way Relay Channels With Multiple Antennas," IEEE Trans. Wireless Commun., vol. 13, pp. 4273-4282, 2014.

[23] J. S. Lemos, F. A. Monteiro, "Full-duplex massive MIMO with physical layer network coding for the two-way relay channel", Proc. IEEE Sensor Array Multichannel Signal Process. Workshop (SAM), pp. 1-5, Jul. 2016.

[24] T. Peng, Y. Wang, A.G. Burr and M. S. Bahaei, "A Physical Layer Network Coding Design for 5G Network," IEEE Global Commun. Conf. (GLOBECOM), 1-7, May 2018, Abu Dhabi.

[25] T. Peng, Y. Wang, A.G. Burr and M. S. Bahaei, "Physical Layer Network Coding in Network MIMO: A New Design for 5G and Beyond," IEEE Trans. on Commun. 67 (3), 2024-2035, Nov. 2018.

[26] A. Burr and D. Fang, "Linear physical-layer network coding for 5G radio access networks," in Proc. IEEE 1st Int. Conf. 5G Ubiq. Connec., pp. 116-121, Nov. 2014.

[27] B. Okyere, L. Musavian, R. Mumtaz "Multi-User Massive MIMO And Physical Layer Network Coding," in Proc. IEEE 7th Int. Workshop Research Adv. in Future Net. Techn., Dec 2019, Globecom, Hawaii.

[28] F. A. P. de Figueiredo, J. P. Miranda, F. L. Figueiredo, F. A. C. M. Cardoso, Uplink performance evaluation of massive MU-MIMO systems, Mar. 2015, [online] Available: https://arxiv.org/abs/1503.02192.

[29] A. J. Viterbi, "An Intuitive Justification and a Simplified Implementation of the MAP Decoder for Convolutional Codes," IEEE J. Select. Areas Commun., vol. 16, pp. 260-264, Feb. 1998.

[30] L. Shi and S. C. Liew, "Complex Linear Physical-Layer Network Coding," in IEEE Transactions on Information Theory, vol. 63, no. 8, pp. 4949-4981, Aug. 2017.